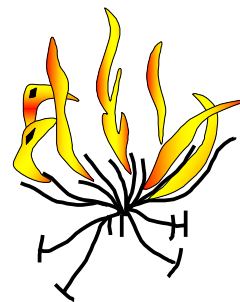




Geological Society of Zimbabwe



Field Trip to Magondi Belt

Sharad Master

28th November 2009

8am Meet at Chinhoyi Cave Motel
Alaska open pit
Deweras aeolianites near Angwa Mine (oldest desert in the world!)
Lomagundi Group road traverse on Lomagundi College Road- Lower Dolomite
Pock-marked Quartzite
Upper Dolomite with stromatolites
Striped Slates
Lomagundi/Piriwiri agglomerates at Nyamakari
Highbury Impact Structure
Mhangura open pits and surface geology
Archaean Eldorado Conglomerates in the Manyame River

Abridged Guide Inside

**IGCP PROJECT 363:
LOWER PROTEROZOIC OF SUB-EQUATORIAL AFRICA**

Post-Conference Field Excursion No 2:
The Palaeoproterozoic Magondi Mobile Belt, NW Zimbabwe

25-30 September 1996

EXCURSION GUIDE

compiled by

Sharad Master¹

*(¹ Economic Geology Research Unit, Department of Geology,
University of the Witwatersrand,
P/Bag 3, WITS 2050, Johannesburg,
South Africa)*

Excursion Leader:

Sharad Master (WITS)

_____oOo_____

INTRODUCTION AND OUTLINE OF GEOLOGY

The Magondi Supergroup is a mainly metasedimentary succession, with minor mafic and intermediate to felsic metavolcanics, which is found in the early Proterozoic Magondi Mobile Belt of western Zimbabwe (Figs. 1 & 2). It is subdivided into the Deweras, Lomagundi and Piriwiri groups, which were deposited between ca. 2.1 and 2.0 Ga (Pb-Pb, Rb-Sr), and metamorphosed between ca. 2.0 and 1.8 Ga (Table 1, after Treloar, 1988). In addition, lithologies of the Dete-Kamativi Inlier of NW Zimbabwe are also part of the Magondi Supergroup. The Magondi Supergroup is underlain by a Basement Complex consisting of Archaean granite-greenstone terrain (including a calc-alkaline magmatic arc succession) and gneisses of the Zimbabwe craton, and the earliest Proterozoic Great Dyke and related complexes that are intrusive into the Archaean rocks.

The Deweras Group, which unconformably overlies the granite-greenstone terrain of the Archaean Zimbabwe craton, comprises a redbed sequence, up to 1.3 km thick, of meta-arenites, rudites, pelites and minor carbonates and evaporites, together with enriched sub-alkaline mafic lavas and pyroclastic rocks. In the northern area, the Deweras Group is subdivided into the Mangula, Norah, Suiwerspruit and Chimsenga formations (Fig. 3). The Deweras Group was deposited in a continental strike-slip basin (Fig. 4), which has been compared with the Dead Sea strike-slip system (Master, 1995).

The Lomagundi Group, which overlies the Deweras Group unconformably, is subdivided into three formations (Fig. 5). The Mcheka Formation consists of basal conglomerates, grits and quartzites, followed by stromatolitic dolomites, phyllites, pockmarked quartzites, argillites and banded iron-formations.

The Nyagari Formation consists of striped slates, sandstones and intermediate volcanics, while the Sakurgwe Formation consists predominantly of greywackes. The overlying Piriwiri Group, which is considered the contemporaneous distal facies equivalent of the Lomagundi Group, is subdivided into three formations (Fig. 6). The Umfuli Formation consists of basal graphitic and pyritiferous slates with narrow bands of cherty manganiferous quartzite, followed by argillites and phyllites with minor interbedded greywackes. The Chenjiri Formation consists of phyllites and greywackes, with minor quartzites, chert, felsites, tuffs, agglomerates and andesites. The Copper Queen Formation consists of a monotonous sequence of phyllites and micaceous feldspathic quartzites, with a ferruginous marble near the base together with major stratiform Cu-Zn-Pb-Fe-Ag massive sulphides.

The tectonic setting of the Magondi Supergroup was in a rift-related continental back-arc basin which formed behind a magmatic arc produced by eastward subduction of oceanic lithosphere under the Zimbabwe craton (Fig. 7). The Magondi Supergroup was deformed into a thin- and thick-skinned fold-thrust belt and metamorphosed from greenschist to granulite facies during the ca. 2.0-1.8 Ga (Rb-Sr, K-Ar) Magondi Orogeny, which resulted from collision of the magmatic arc and closure of the back-arc basin. The western part of the Magondi belt was affected by tectonothermal events

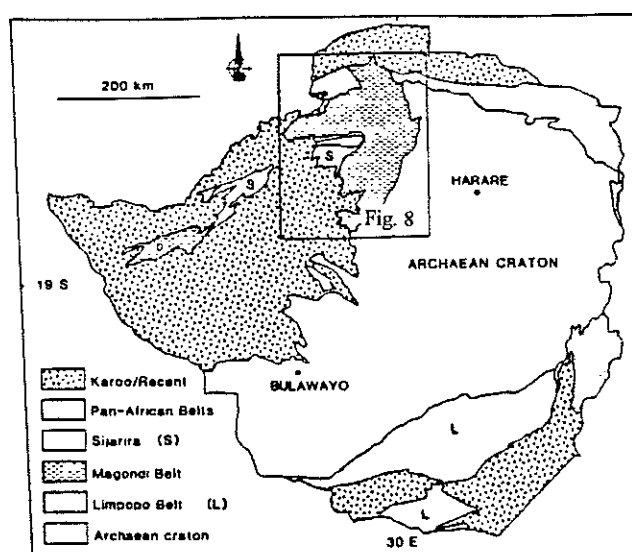


Figure 1: Simplified geological map of Zimbabwe showing the Magondi Belt positioned to the NW of the Archaean craton. The box indicates the position of Fig. 8.

Table 1: Geochronology of the Magondi Belt and related basement units (after Treloar, 1988).

Age (Ma)	Data	Event
400-650	K-Ar mica ages	Pan-African Zambesi thermal event
1659 (50)	K-Ar Piriwiri slates	Magondi metamorphic age
1753 (65)		
1905 (70)		
1974 (70)		
1780 (280)	Rb-Sr Piriwiri granulites, Nyaodza	Magondi metamorphic age
1890 (280)	Rb-Sr Piriwiri granulites, Rukomeshe	Magondi metamorphic age
1980 (80)	Rb-Sr WR granites (includes Urungwe granite	Syn- to post-tectonic granites
2153 (125)	Rb-Sr WR Urungwe granite but note: 1211 (40) muscovite Rb-Sr 948 (40) muscovite K-Ar	Syn- to post-tectonic granite
2150 (100)	Rb-Sr pegmatites and late granites. Dett	Post-tectonic granites
2100 (200)	Pb-Pb galenas (Piriwiri Copper Queen massive sulphide)	Sedimentation age
2170 (100)	Rb-Sr basal Deweras lavas	Sedimentation age
2360 (90)	Rb-Sr Chipisa paragneisses	} Early Proterozoic crustal forming event
2465 (53)	Rb-Sr Kariba paragneisses	
2460	Great Dyke	End Archaean

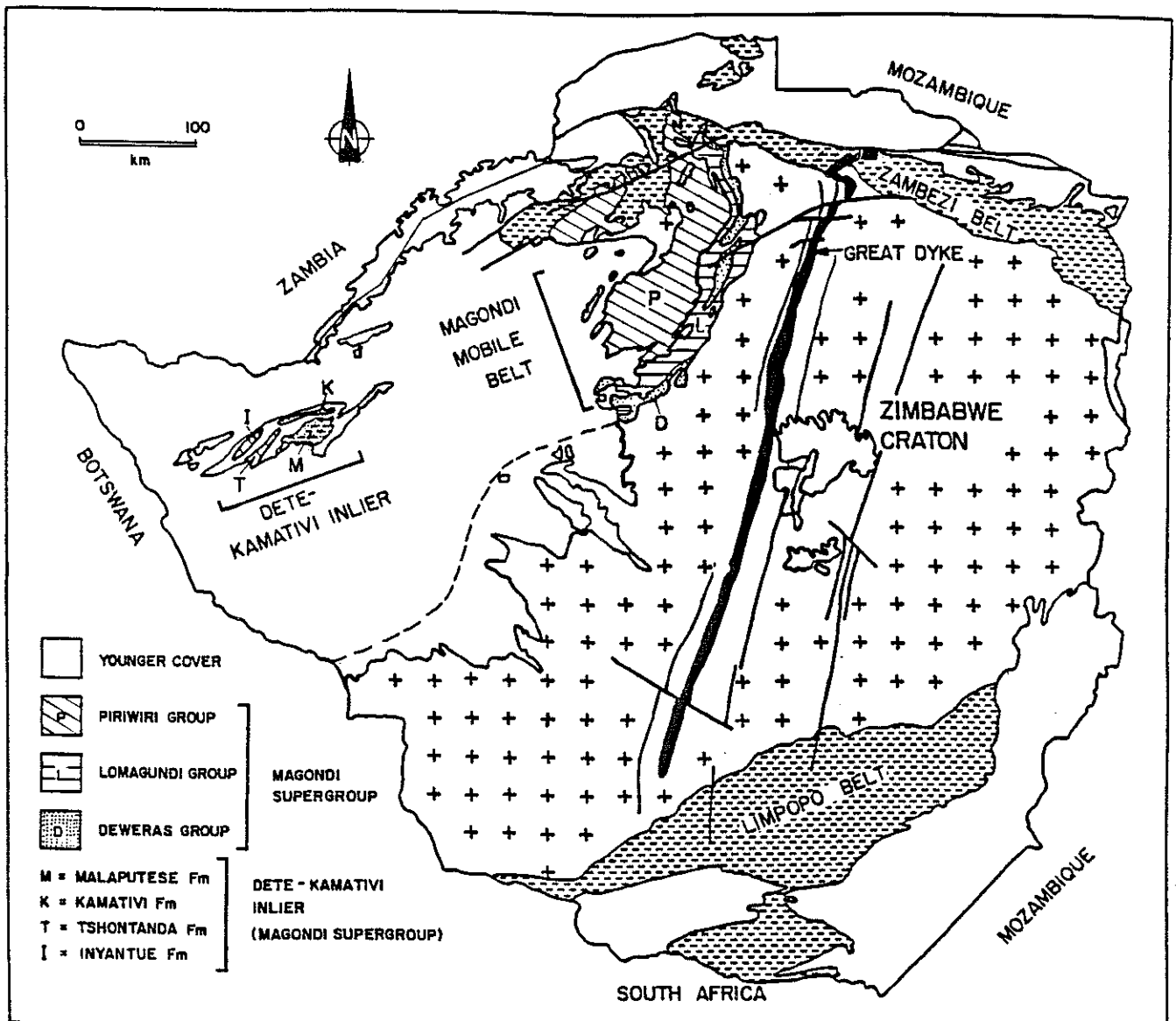


Figure 2: General map of Zimbabwe, showing the Magondi Supergroup and the Magondi Mobile Belt in relation to the Archaean Zimbabwe Craton and the Limpopo and Zambezi Mobile Belts. Note the fracture system on the Zimbabwe Craton, occupied by the Great Dyke and its satellite intrusions, which is parallel to the trend of the autochthonous Deweras Group in the Magondi Basin.

(after Master, 1991)

DEWERAS GROUP (Northern Facies)

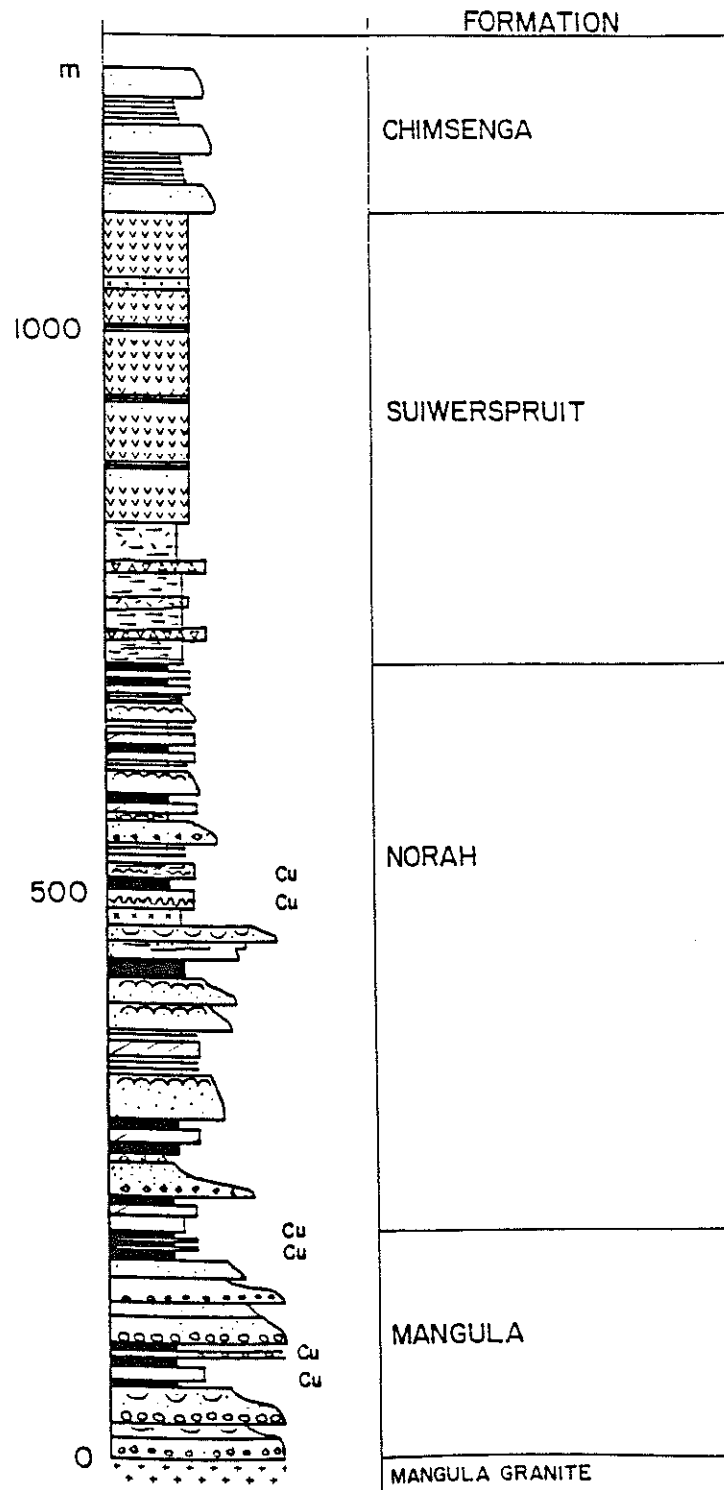
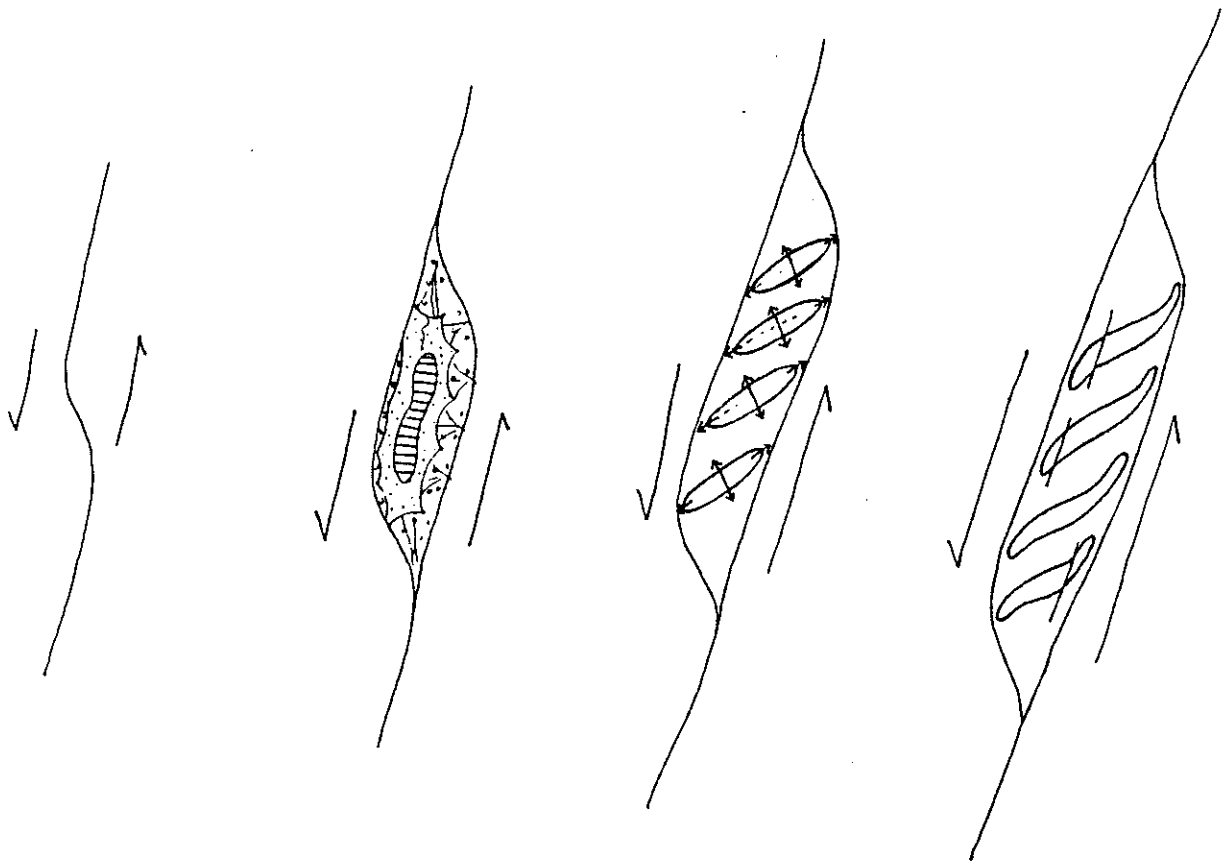


Figure 3: Generalised lithostratigraphy of the northern part of the Deweras Group (after Master, 1991)



TECTONIC SETTING OF THE DEWERAS GROUP

Figure 4: Tectonic setting of the Deweras Group: (a) releasing bend on sinistral strike-slip fault of the Great Dyke-Popoteke fault set, (b) Deweras Group sedimentation in a strike-slip basin, (c) formation of en echelon doubly-plunging synsedimentary anticlines, (d) sigmoidal recurving of the en echelon anticlines into shear direction, and cutting through of wrench faults.

(after Master, 1991) :

LOMAGUNDI GROUP

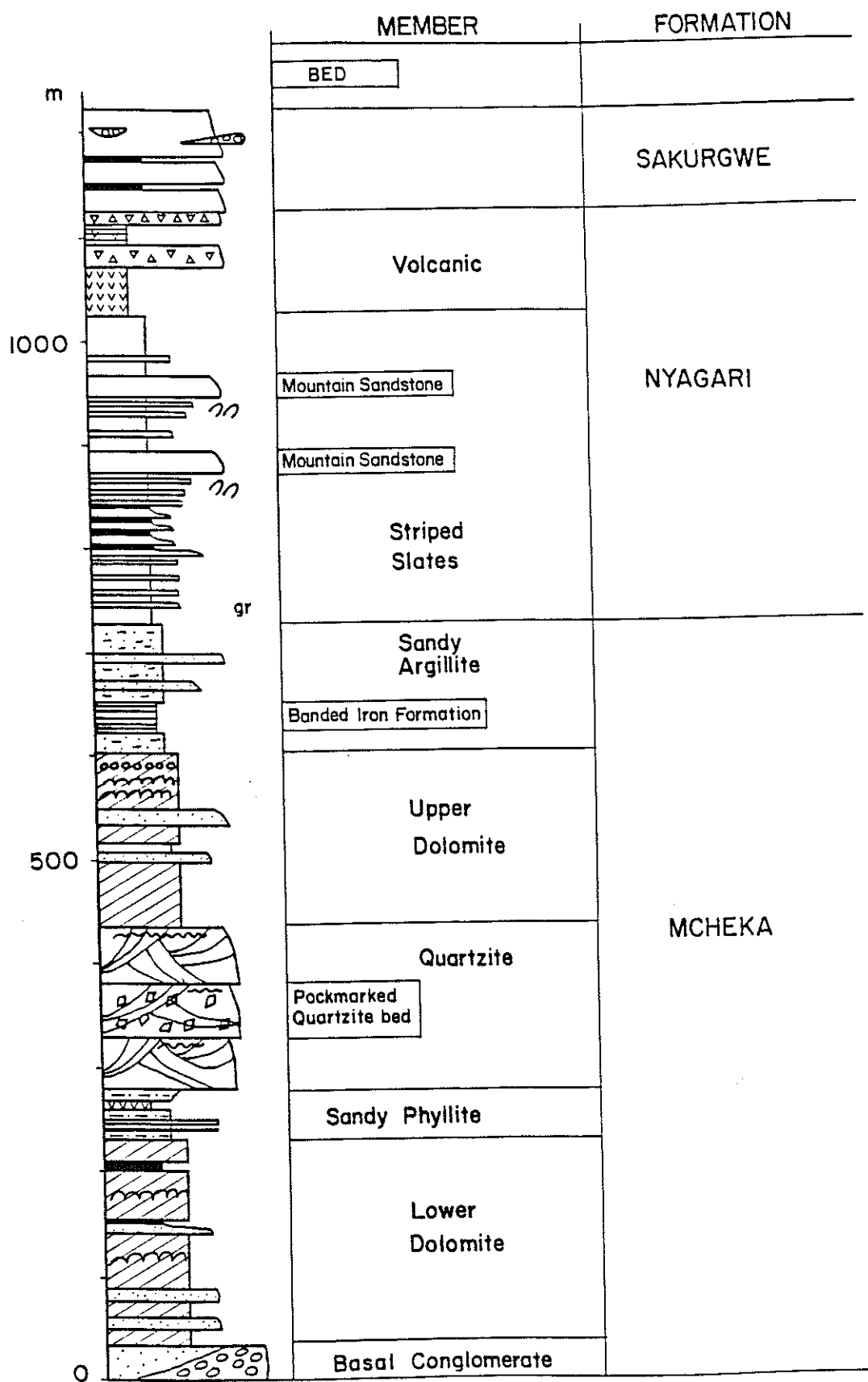


Figure 5: Generalised lithostratigraphy of the Lomagundi Group

(after Master, 1991)

PIRIWIRI GROUP

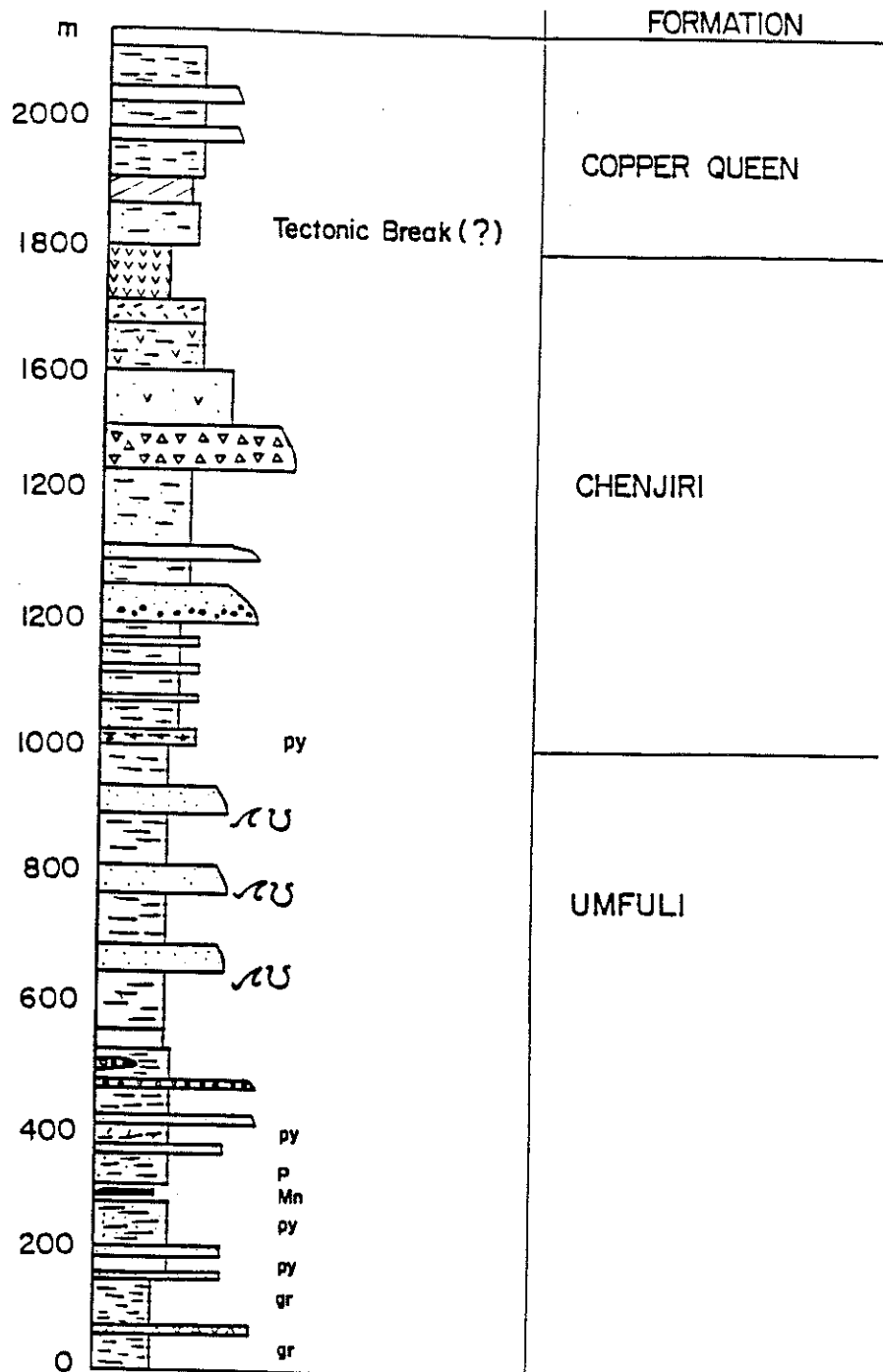
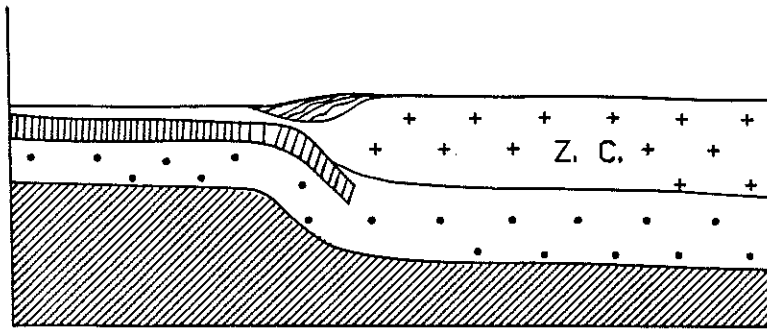


Figure 6: Generalised lithostratigraphy of the Piriwiri Group

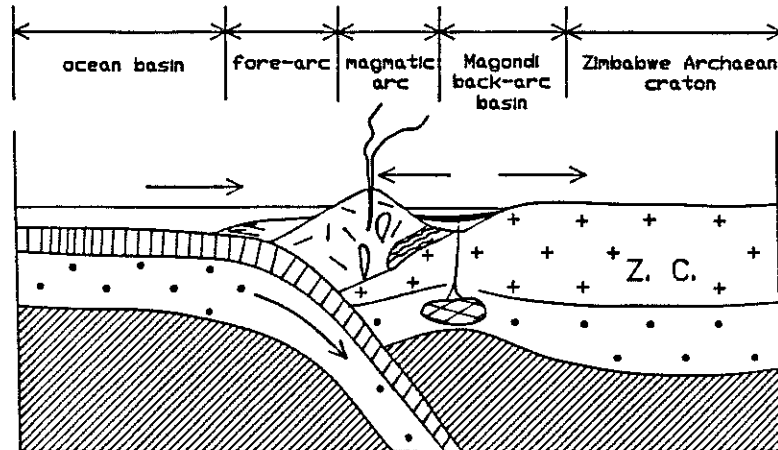
(after Master, 1991)



c. 2.2 Ga

Initiation of Subduction

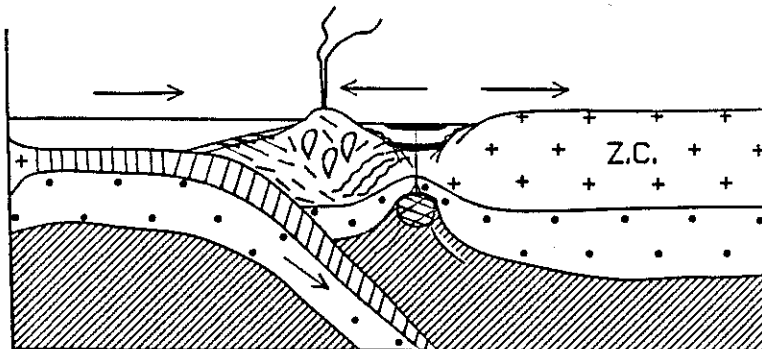
Thrusting and accretion of Kariba paragneisses on craton margin.



c. 2.1 Ga

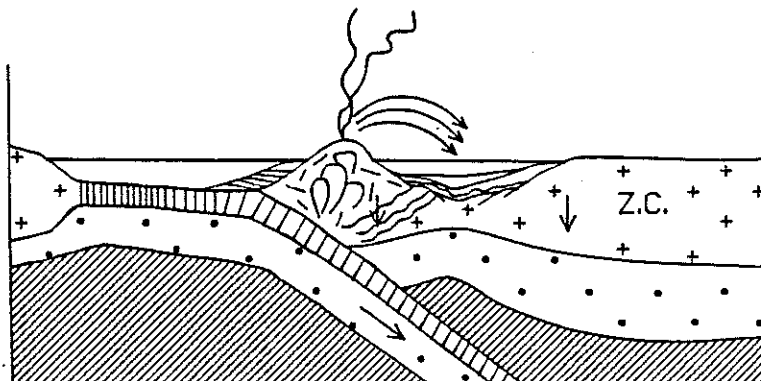
Early back-arc rifting

Deweras Group basalts with I-type-MORB characteristics (mixed lithospheric source)



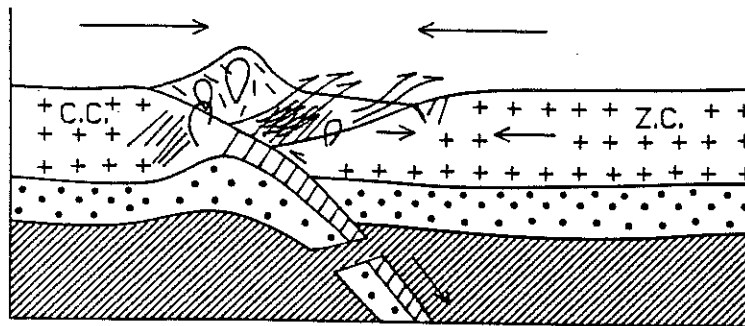
Later rifting

Deweras Group basalts with P-type-MORB characteristics (asthenospheric mantle plume source)



Thermal subsidence stage

Lomagundi & Piriwiri Group deposition. Calc-alkaline volcanic and pyroclastic input into basin from magmatic arc.



c. 1.8 Ga

Collisional stage

Magondi orogeny.

Magmatic arc thrust over back-arc basin. Back-arc basin sequence thrust onto Zimbabwe craton.

//// = granulite metamorphism

Key.

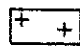
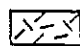






-  Continental crust : Z.C. = Zimbabwe craton
C.C. = Congo craton
-  Juvenile magmatic arc.
-  Oceanic crust.
-  Lithospheric mantle.
-  Juvenile plutons.
-  Source region for Deweras Group volcanics.
-  Kariba paragneisses.
-  Asthenospheric mantle.

Figure 7: Schematic summary of the evolution of the Magondi Basin between 2.2 to 1.8 Ga, from the initiation of back-arc rifting, and the deposition of the Deweras, Lomagundi and Piriwiri Groups, to the Magondi Orogeny.

(after Master, 1991)

related to the mid-Proterozoic (1.3-0.9 Ga) Irumide Orogeny, and was also affected by the Pan-African (850-550 Ma) Zambezi Orogeny.

The Magondi belt was unconformably overlain by middle and late Proterozoic rocks of the Sijarira and Makuti Groups, which were deformed and meta-morphosed in the late Proterozoic to early Palaeozoic Pan-African Zambezi Orogeny. Post-orogenic molasse of Ordovician age was deposited in the Mid-Zambezi valley area. Following Pan-Gondwana glaciation, Permian and Triassic Karoo Supergroup rocks were deposited in rift basins in the Middle and Lower Zambezi Valley areas. This culminated with extensive Karoo flood basalt volcanism in the early Jurassic. Post-Karoo rifting initiated in the late Jurassic, and has carried on to the present day in the Zambezi Valley, which is still seismically active. Large areas of western Zimbabwe are covered with Permo-Triassic and Jurassic deposits, as well as by Tertiary and Quaternary aeolian deposits of the Kalahari. These younger deposits obscure the underlying rocks of the Magondi Belt, which is only exposed in the northwest, and in the Dete-Kamativi inlier in the west.

Excursion Stops

Day 1.

Stop 1 (Fig. 8): Kariba Dam Wall

Exposures of Kariba paragneisses, including "Kariba sillimanite quartzite"

In the northern part of the Magondi Belt, the basement consists of a succession of para- and orthogneisses which have been considered part of the "Zambezi Belt" (Thole, 1976; Broderick, 1981). These gneisses, which include the Urungwe, Escarpment, Chiroti, Chipisa, Kariba, Chitumbi, Mazamo and Chinemba gneisses, are extremely variable in texture and composition, and vary from foliated granitic leucogneisses to biotite gneisses to migmatites. There are also intercalations of hornblende-diopside calc-silicate gneisses. Some of the gneisses are associated with plugs and sills of tremolite-chlorite rock and para-amphibolites which are interpreted as metamorphosed volcanic tuffs (Thole, 1974). Granitoids consisting of plugs of granodioritic and tonalitic gneisses intruding the various paragneiss units have been recorded by Hitchon (1958), Wiles (1961), Loney (1969), Broderick (1976), Chenjerai (1988) and Bartholomew (in prep.). Granitic gneisses (the Tengwe and Kwetchi granites) have been described from the southern Hurungwe (Urungwe) area by Harper (1973). In the Copper Queen area, Leyshon (1973) has described several Pre-Magondi basement inliers (Copper Queen and Copper King domes), consisting of biotitic quartzo-feldspathic granite-gneiss which have been intruded by weakly foliated granites. A meta-granite in the Kariba area which is intrusive into paragneisses, was dated by Loney (1969) at 2050 ± 32 Ma (recalculated Rb-Sr whole rock). The Chipisa Paragneisses were dated by Loney (1969), and have yielded a recalculated age of 2443 ± 90 Ma. This imprecise result indicates a late Archaean to early Proterozoic age for the metamorphism that affected

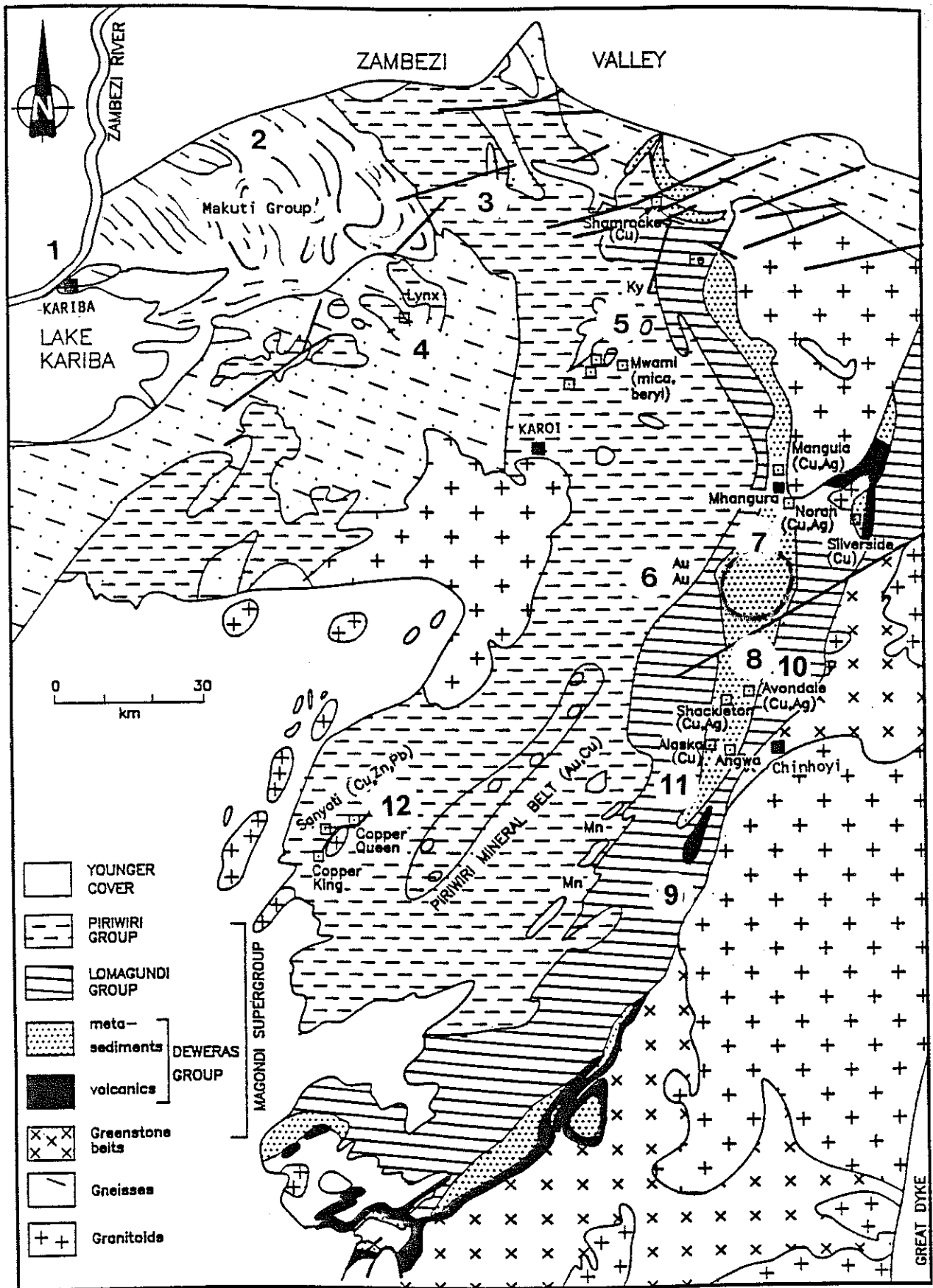


Figure 8: Geological map of the northern part of the Magondi Belt, showing the main excursion stops, and the location of the principal mines and mineral deposits hosted by rocks of the Magondi Supergroup (after Master, 1991).

these rocks. There are also some recent indications from U-Pb dating on zircons that the Chipisa gneisses are Late Archaean in age (Munyanyiwa and Kröner, unpubl. Data; pers. comm.)

The Kariba Paragneisses are a northern continuation of the Chipisa Paragneisses, and also consist of foliated biotite paragneisses with calc-silicate bands and thin leucogneisses (Hitchon, 1958; Loney, 1969; Kirkpatrick and Robertson, 1987; Broderick, 1976). There are also some porphyroblastic biotite gneisses containing euhedral microcline and microperthite porphyroblasts, which are associated with small plugs of adamellite and granodiorite (Hitchon, 1958; Broderick, 1976). Sillimanite quartzites occur interbedded within the Kariba Paragneisses, and are regarded as an arenaceous facies of the paragneiss. Loney (1969) obtained a (recalculated) age of 2368 ± 92 Ma for the Kariba Paragneisses. This imprecise age records the metamorphism, and must be regarded as a minimum age. The age of sedimentation of the protoliths is unknown, but was most probably late Archaean.

The paragneisses and their associated intrusive granitic orthogneisses and ortho-amphibolites record a major orogenic cycle that is imprecisely dated, but predates the 2.1 Ga Magondi Supergroup. Because most of the gneisses occur in the Hurungwe District, and occupy an area that has been termed the 'Urungwe Subprovince' (Stowe et al., 1984), it was proposed by Master (1991) to call this orogenic cycle the Hurungwe Orogeny. The age constraints on this orogenic cycle are very poorly defined. The only dating of the paragneisses, by Loney (1969), indicates ages that span 2533 to 2276 Ma, i.e. late Archaean to early Proterozoic. Since the gneisses of the Hurungwe District can be correlated with the gneisses in the Guruve (Sipolilo) District, as appears probable from the mapping of Hahn et al. (1990), they must be late Archaean in age, since the Guruve gneisses were intruded by the 2470 Ma old Great Dyke (Worst, 1960; Wiles, 1968, 1972; Prost, 1982).

Interpretations of the metasedimentary paragneisses indicate that they were deposited in a marine environment. The biotitic and quartzo-feldspathic leucogneisses of the Urungwe and Escarpment Paragneisses may have been arkoses and greywackes, and together with the intercalated para-amphibolites (metamorphosed marls), may have been deposited in a shallow marine setting. In the overlying paragneisses, the lack of coarse clastic material, major carbonate units or arenites rules out a near shore or shallow shelf setting, and indicates a deeper marine depository. Thick sequences of fairly uniform biotite gneisses in the Chipisa Paragneiss may be meta-turbidites, and may have been deposited in a deep-sea fan setting similar to the Kuiseb Schists of the Khomas Trough in the Damara Belt (Kukla and Stanistreet, 1990).

The Hurungwe orogenic cycle may have involved subduction of oceanic crust underneath the Zimbabwe craton, with orogenic obduction of an accretionary wedge onto the western edge of the craton. If a latest Archaean age is accepted for the protoliths of the Hurungwe gneisses, then they may have been contemporaneous with the calc-alkaline rocks of the Bulawayan Upper Greenstones in the western part of the Archaean craton,

for which a subduction related origin has been proposed by Condie and Harrison (1976), Wilson et al. (1978) and Watkeys (1984). In Watkeys' (1984) scheme, the Upper Greenstones represent an Andean-type magmatic arc, produced by eastward oblique subduction of oceanic crust as the Zimbabwe craton moved south-westward before colliding with the Kaapvaal craton in the Limpopo Mobile Belt. The Hurungwe belt of paragneisses may then represent a fore-arc trench complex formed on the leading edge of the Zimbabwe Archaean craton (Master, 1991).

Stop 2 (Fig. 8): Makuti Group exposures on Zambezi Escarpment

Exposures of the Late Proterozoic Makuti Group (Fig. 9) along the Zambezi Escarpment are flat-lying, but highly deformed and metamorphosed. Good examples of boudinage can be seen in quartzofeldspathic psammitic beds intercalated with pelitic and semi-pelitic schists. Brecciated dolomitic marbles are seen close to the escarpment fault. Munyanyiwa et al. (1996) interpret felsic gneisses and amphibolites from the Makuti Group as representing a bimodal rift sequence in an intraplate setting. Although Munyanyiwa and Blenkinsop (1992) ascribed the basic structure of the Vuti synform (Figs. 9 & 10), to two phases of deformation, more recent evidence suggests that there was an earlier phase of deformation that preceded their D1 event. This is manifested by the presence of an early schistosity that is folded by D1 folds, and possibly by rootless isoclinal folds, both in the Makuti Group (T.G. Blenkinsop, pers. comm., 1996).

Stop 3 (Fig. 8): Rukomeche River enderbites.

These granulites are metamorphosed equivalents of Piriwiri Group rocks, and have been dated by Treloar and Kramers (1989) at 1890 ± 260 Ma.

Stop 4 (Fig. 8): Lynx Graphite Mine.

The graphitic schists of the Piriwiri Group have in places been highly deformed and metamorphosed to high grades, and the resulting flake graphite has been exploited at the Lynx Graphite Mine and in several smaller prospects (Muchemwa, 1987) (Figs. 11 & 12). The mineralization at Lynx Graphite Mine is confined to a horizon of graphite schist which is interbedded with sillimanite and biotite gneisses and feldspathic psammites (Armstrong, 1975). The graphitic horizon has been traced geophysically and by trenching for a strike length of over a kilometre (Davies, 1982; Muchemwa, 1987).

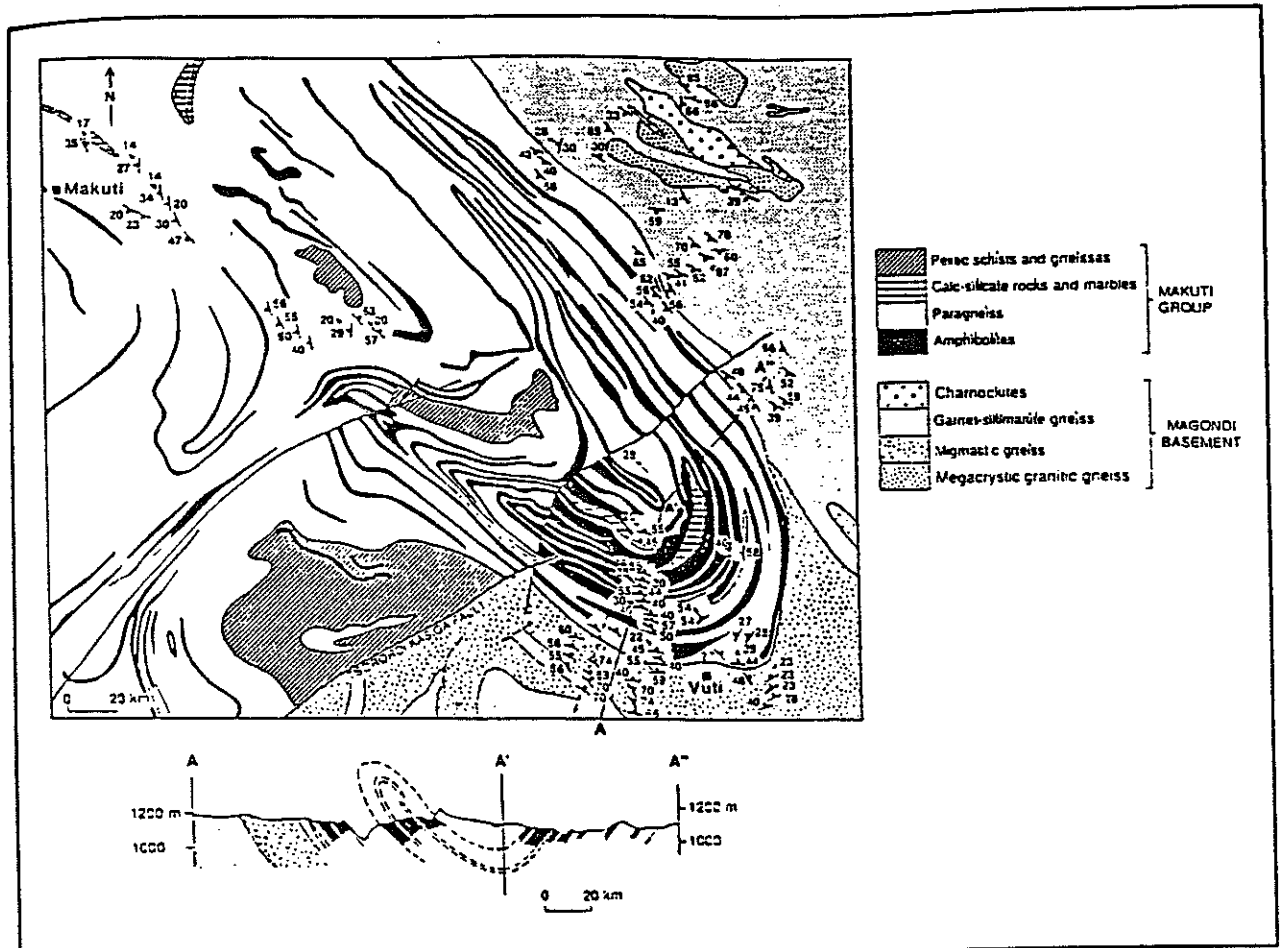


Figure 9: Geology of the Makuti Group and the underlying basement in the Vuti synform (after Munyanyiwa & Blenkinsop, 1992). Cross section A-A' shows refolding of the basement rocks.

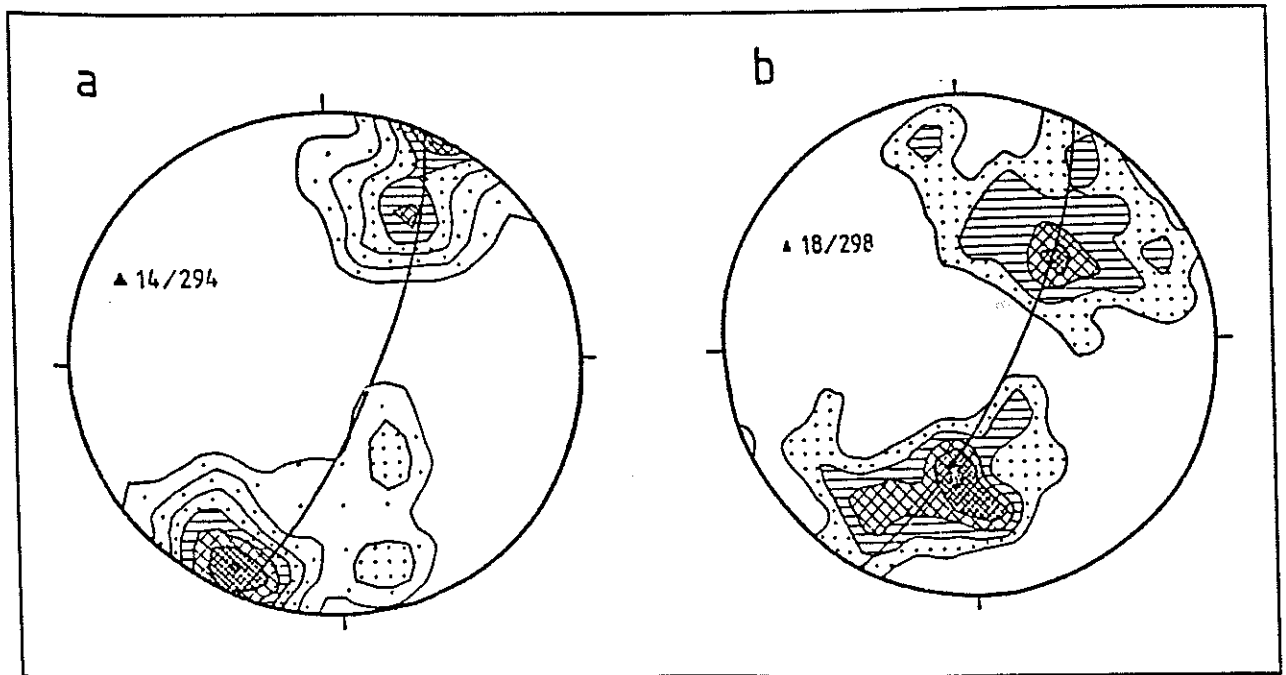


Figure 10: Lower hemisphere equal area contoured stereoplots of poles to (a) Magondi basement foliations (n=55); (b) Makuti Group foliations (n=131). Great circle is best-fit great circle, with plunge and bearing of plunge (after Munyanyiwa & Blenkinsop, 1992).

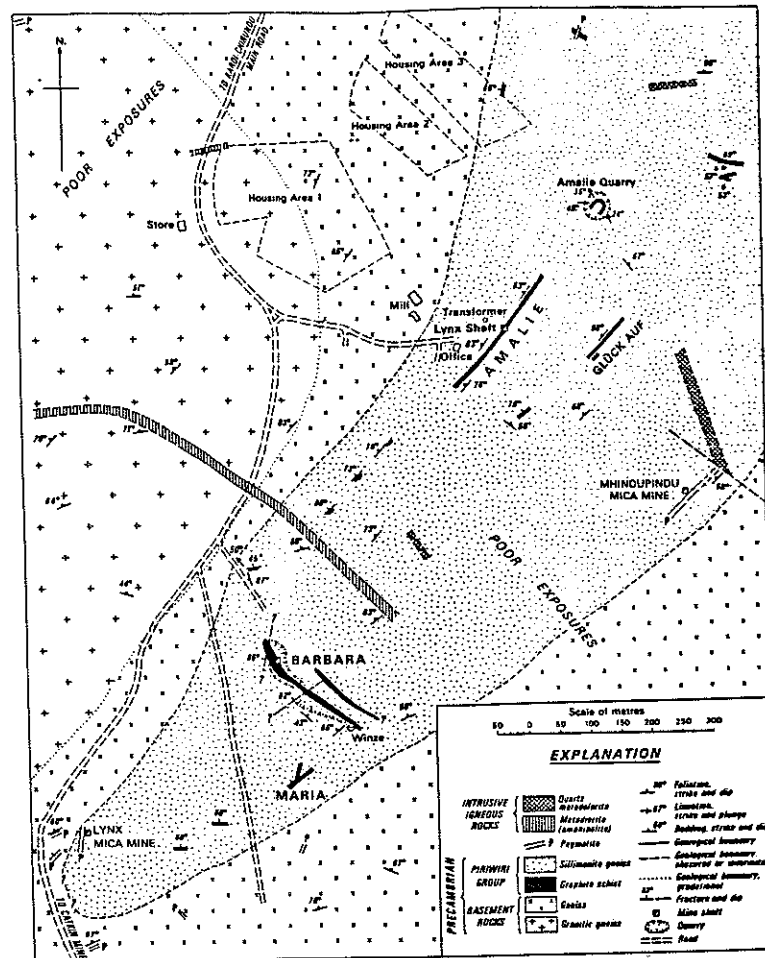


Figure 11: Geological map of the Lynx Graphite Mine (after Armstrong, 1975; and Muchemwa, 1987)

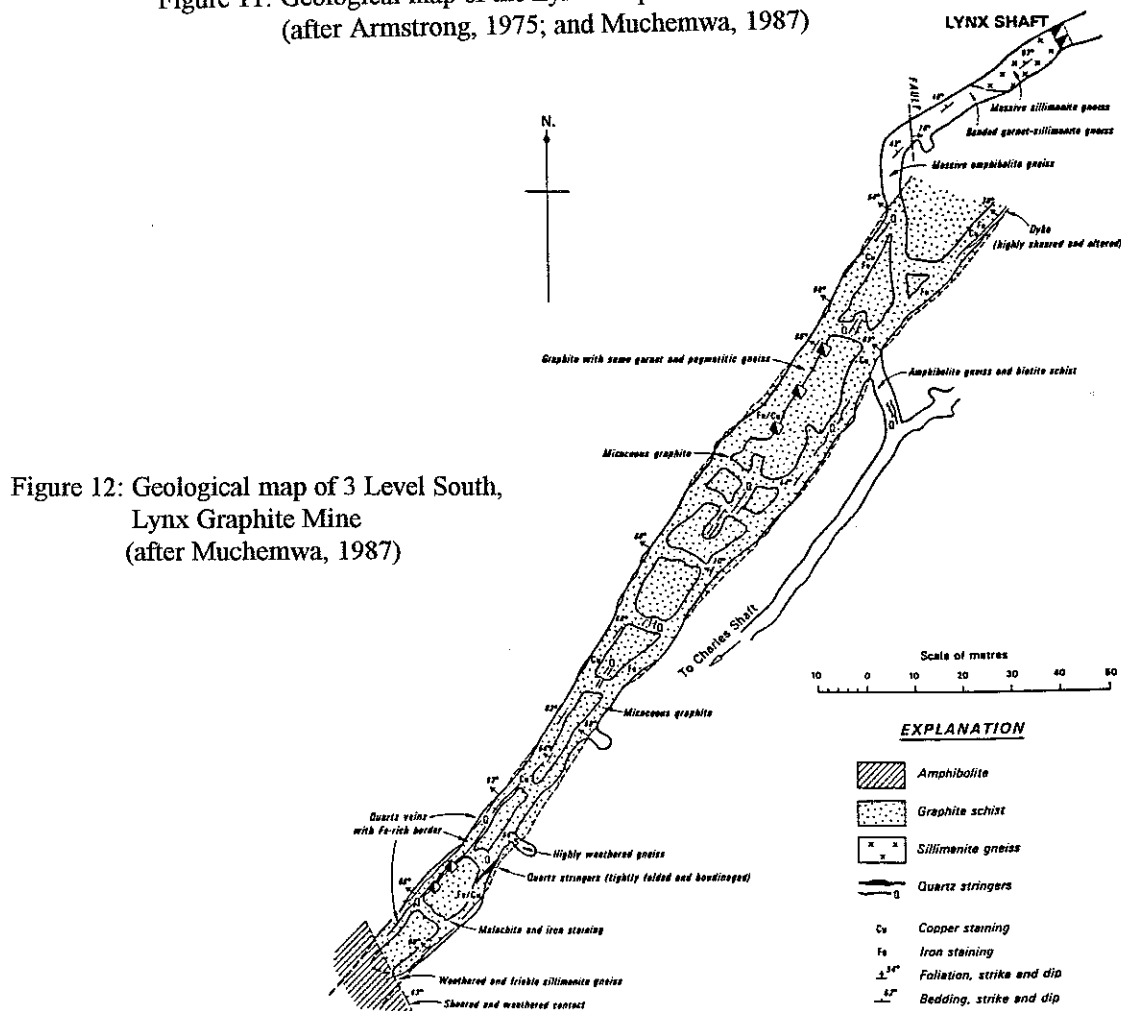


Figure Geological map of 3 level south, Lynx Graphite Mine

Day 2

Stop 5 (Fig. 8): Mwami (Miami) mica field

5.1 The Mwami mica field contains muscovite mica pegmatites (Figs. 13 & 14, after Wiles, 1961) related to regional metamorphism of the Piriwiri Group (Fig. 15). There are also mica and beryl pegmatites (with gem tourmaline and blue topaz) related to intrusive Miami granites (Pan-African age) (Fig. 16, after Treloar, 1998).

5.2: Masterpiece Farm kyanite deposit

This is a deposit situated in a belt of Piriwiri Group graphitic schists, in which kyanite pseudomorphs after andalusite (chiastolite) occur (Fig. 17). The kyanites, which occur as single crystals and penetration twins (Figs. 18 a & b), were described by Workman and Cowperthwaite (1963).

Stop 6 (Fig. 8): D-Troop cluster of Au deposits along the Angwa River

6.1. The D Troop mine is one of several small gold mines and prospects along the Angwa River, in which gold mineralization is associated with a stockwork of N-trending quartz veins cutting phyllites and more sandy argillites of the Piriwiri Group. The veins appear structurally related to a NE-plunging anticline with minor drag folds. The gold is associated with pyrite. Most of the workings are shallow, and are confined to the oxide zone. The cumulative production from 1892 to 1984 was 556.22 kg Au at an average grade of 4.2 g/t (Bartholomew, 1990).

The D Troop mine is one of the most ancient authenticated mines in Zimbabwe. In the 1890's, when the old diggings were opened up by prospectors, an engraved bronze cup was found in the workings. This cup, which is now in the National Museum in Bulawayo, contains incised Indian designs which have been dated to ca. the 14th Century AD, i.e., during the height of the gold-based Monomotapa kingdom, which was centred on Great Zimbabwe.

In the 16th Century, the Portuguese had taken control of the coastal areas of Mozambique, and took over the gold trade that was formerly run by Arabs based in the sultanates of Zanzibar, Pemba and Chilwa off the coast of East Africa. The Portuguese penetrated inland up the Zambezi and its tributaries, and built forts along the Angwa River, from where they controlled the gold mines of the D Troop cluster.

Figure 14: Idealised plans of pegmatites from the Mwami mica field

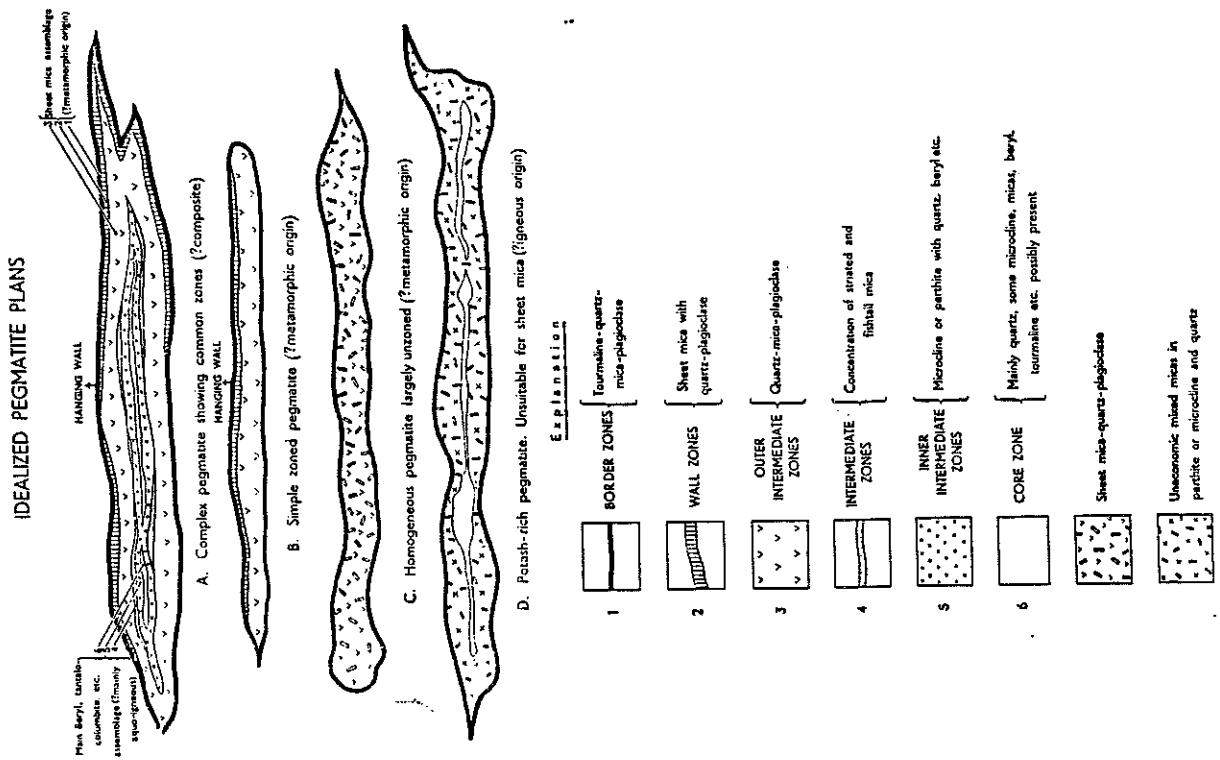
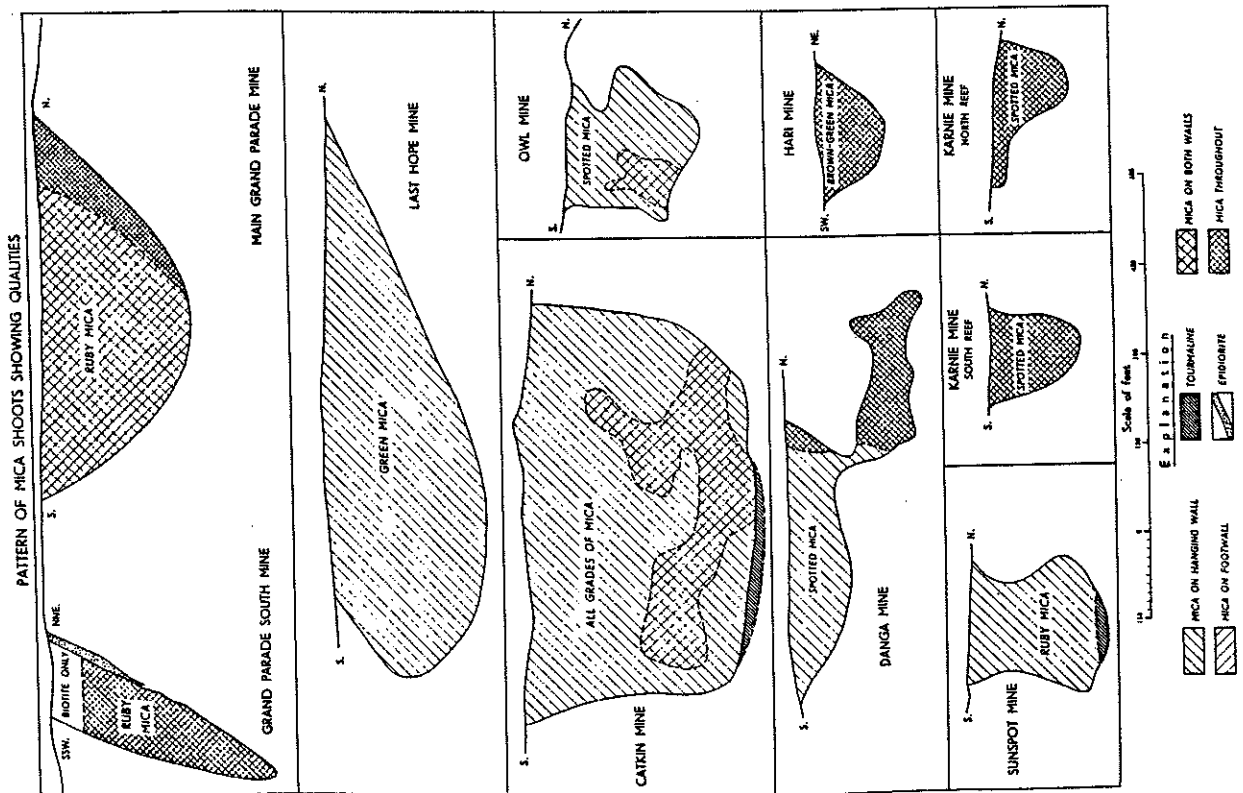


Figure 13: Longitudinal sections of mica shoots from the Mwami mica field (after Wiles, 1961)



(after Wiles, 1961)

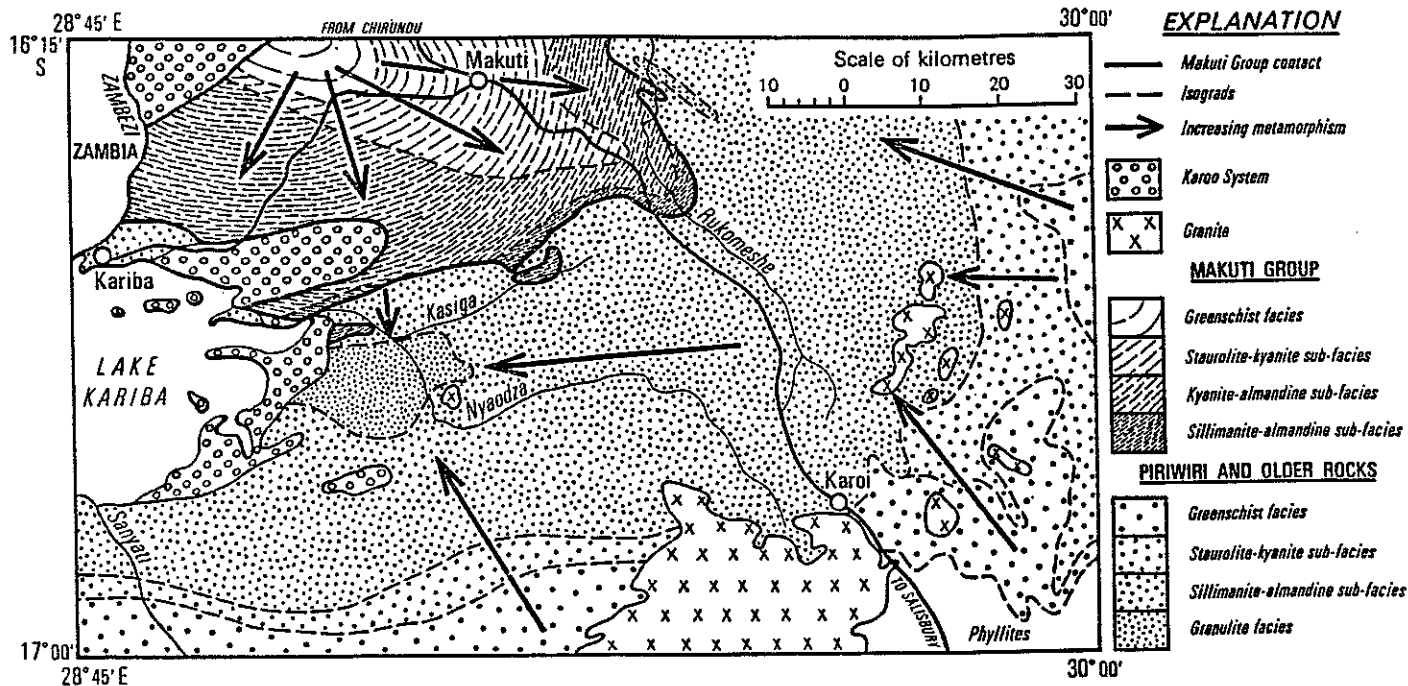


Fig. 15: Regional metamorphism around Makuti, Karoi and Kariba (after Broderick, 1976).

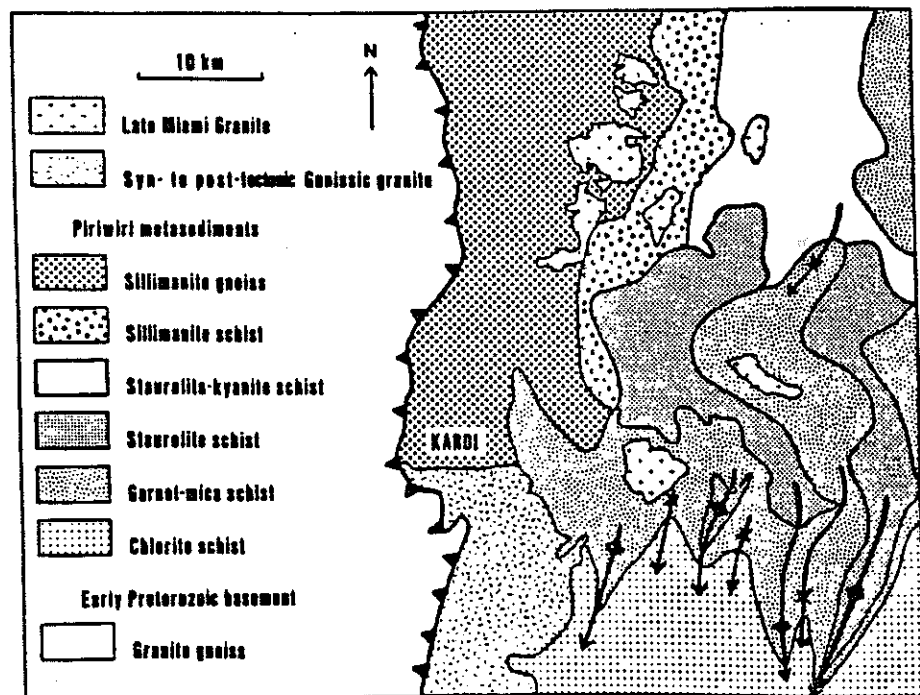


Fig. 16: Metamorphic map of the Mwami area (after Wiles, 1961; Treloar, 1988), showing post-metamorphic folding of the metamorphic isograds, and the late Miami Granite.

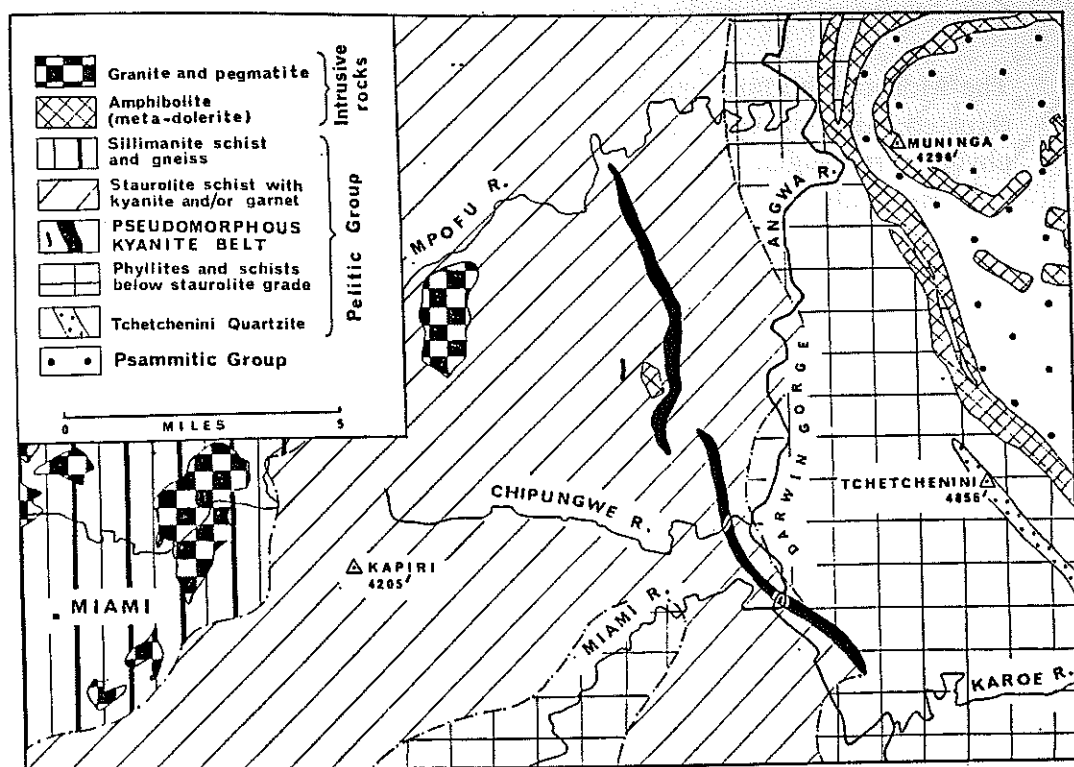


Fig. 17: Generalised geological map of the country east of Mwami, showing belt of pseudomorphous kyanite after chialstolite (after Workman & Cowperthwaite, 1963).

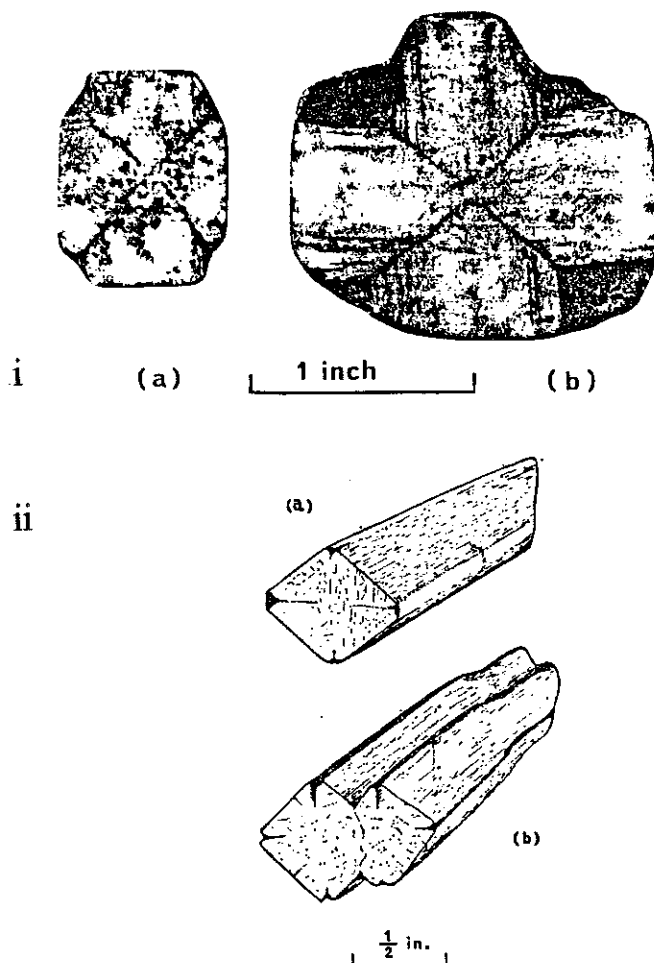


Fig. 18: (i a&b) Examples of chialstolite crystals now entirely converted to kyanite. (iia) a single crystal, (iib) a penetration twin. The specimens have been cut parallel to (001) to show the cross-sections (after Workman & Cowperthwaite, 1963).

6.2: Morocco Manganese Claims.

The Morocco claims, near D-Troop mine, contain manganese oxide mineralization in a thrust zone of argillites separating Lomagundi Group rocks from Piriwiri Group phyllites. Individual bodies, averaging 45 m in length and 60 cm in width, are associated with brecciated concordant quartz veins (Kirkpatrick, 1976). 733 tonnes of ore grading 45% MnO₂ were declared from 1961-1966.

Day 3

Stop 7 (Fig. 8): Mangula Cu-Ag Mine, Mhangura

7.1. Underground visit to Mangula Mine, the largest copper-silver producer in Zimbabwe (Figs. 19-22). Mangula a stratabound sediment-hosted Cu-Ag-Au-Pt-Pd-(U,Mo) deposit hosted in red beds of the early Proterozoic (ca. 2.1 Ga) Deweras Group, which unconformably overlies the Archaean basement. The host rocks are arkoses, conglomerates and metapelites of the Mangula Formation, which were deposited in alluvial fan and braided stream environments. The rocks were deformed and metamorphosed to greenschist facies during the ca. 2.0-1.8 Ga Magondi Orogeny, as well as during the Irumide (ca. 1.3-0.9 Ga) and Pan-African Zambezi (ca. 550 Ma) orogenies.

Although Mangula was discovered in the 1920's, mining only commenced in 1957, and its original size is estimated to have been 60 million tonnes at an average grade of 1.2% copper and 20 g/t silver. Important by-product gold, platinum and palladium are recovered from the ores. Copper mineralization occurs over a stratigraphic thickness of about 200 m in the basal part of the Deweras Group. For mining purposes, the deposit is divided into eight parallel tabular orebodies separated by subgrade mineralization or barren zones, and extending along strike for 2 km. Most of the orebodies coalesce at depth and extend down-dip to about 900 m below surface.

The orebodies at Mangula Mine are hosted by alluvial fan and braided stream lithologies of the Mangula Formation. Although the mineralization is found in all rock types, there is a strong spatial association with lithologies of the distal fan facies association, in particular where there is an interfingering of permeable arkosic horizons with impermeable pelitic beds. The orebodies, which have an elongate tabular form concordant with the bedding, consist of disseminated chalcocite and bornite, with subordinate chalcopyrite and minor pyrite and molybdenite. The footwall of the orebodies are characterised by intense reddish haematitic alteration, accompanied by silicification and microclinization of arkosic arenites. In these zones, sedimentary structures such as cross-bedding are completely destroyed, and replaced by stratiform zones of haematite and magnetite bands and ellipsoids which are parallel to both bedding and cross-bedding. The magnetite ellipsoids may also contain minor copper sulphides and uraninite. The main source of the uranium, as revealed by fission track studies, was detrital zircon (together with minor allanite and apatite), that was concentrated in heavy mineral layers in the sediments. The magnetite ellipsoids have been shown to be flattened triaxial oblate ellipsoids, which are true strain

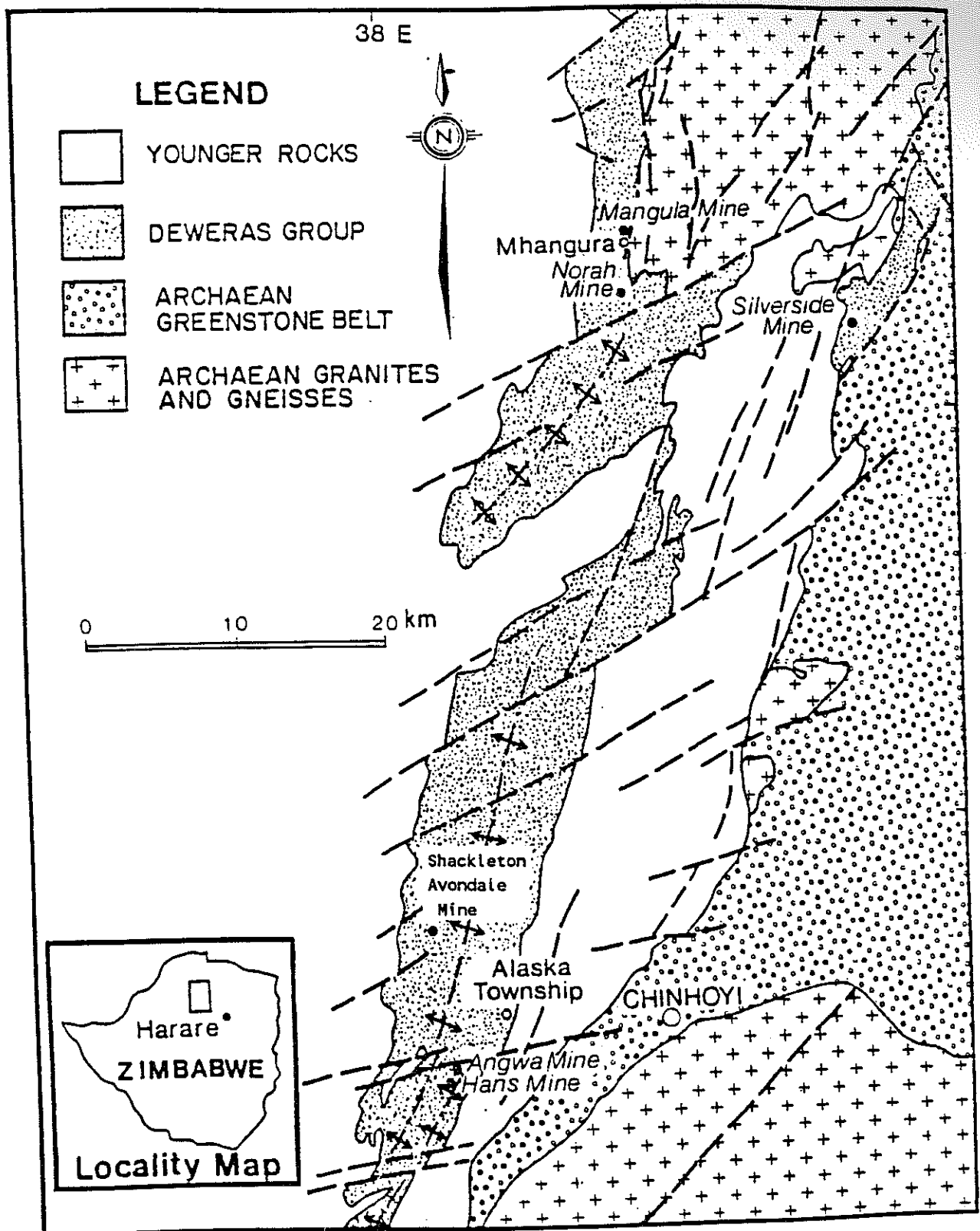
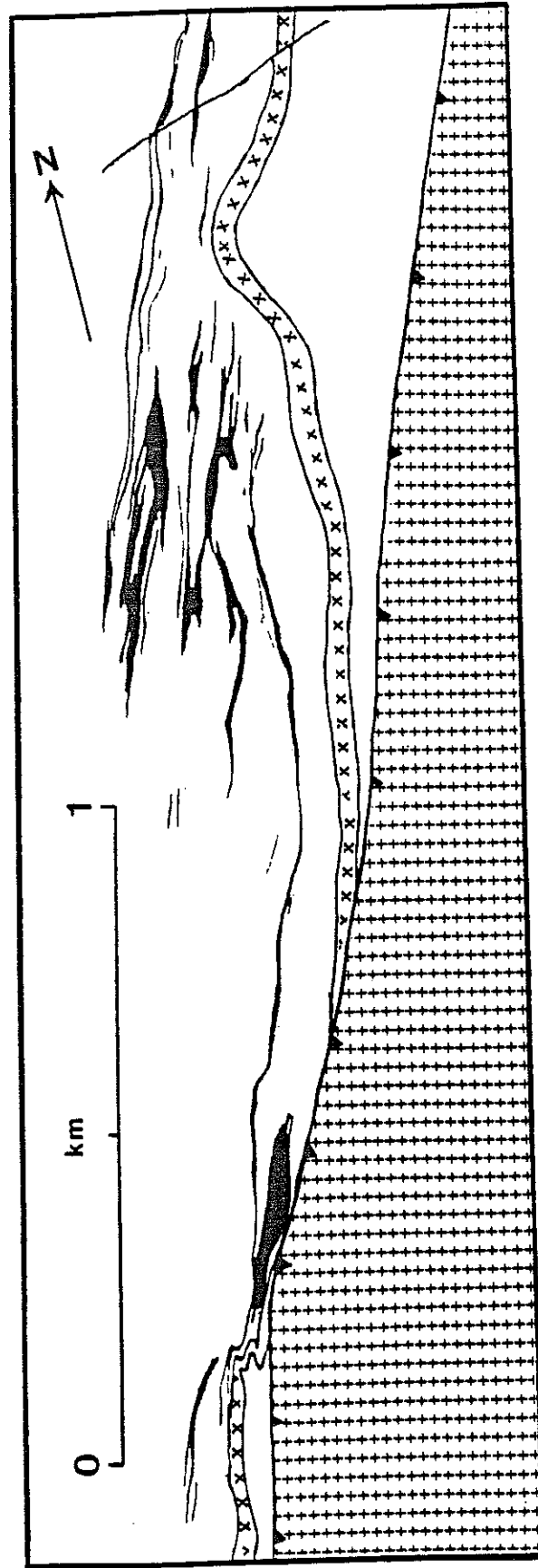


Figure 19: Locality map of the Magondi Copperbelt, showing the Deweras Group in relation to the Archaean granite-greenstone belt basement (after Master, 1991)

Figure 20

Plan of 5-00 Level, MANGULA MINE



+ = Mangula Granite, x = Mangula Metadolerite Dyke, black = orebodies, unornamented =
 Deweras Group metasediments (Mangula Formation)
 (after Master, 1991)

ellipsoids formed by deformation of initially spherical reduction spots which are common in redbeds of all ages (Master, 1991). Oxidising metamorphic fluids generated by pressure solution during the first phase of deformation were responsible for very similar haematite-microcline alteration, especially around faults and veins.

The ore minerals are divided into primary (hypogene) minerals and secondary (supergene) minerals. The main primary sulphide minerals are chalcocite and bornite, with subordinate chalcopyrite and pyrite, minor digenite, molybdenite, and trace acanthite and wittichenite. The primary non-sulphides include native copper, native silver, native gold, magnetite, haematite, rutile, sphene, chromite, and uraninite. Silver and gold also occur as lattice-substitutions in copper sulphides. Platinum and palladium are also recovered as by-products from the sulphides, and no discrete platinum-group mineral has been identified as yet. There is no galena or sphalerite. The secondary minerals, which are restricted to the uppermost, oxidised parts of the orebodies, include malachite, chrysocolla, cornetite and pseudomalachite, together with minor azurite, turquoise, native copper, bornite, digenite, covellite, chalcopyrite, cupriferous wad, metatorbernite, uranophane and chalcantite. There is a very strong correlation between Cu and Ag values, and a good correlation between Ag and Au values in the primary ores (Master, 1991). Au and PGE (Pt, Pd, Ir) are concentrated in sulphides and magnetites, and are highly depleted in the haematized and K-metasomatized alteration zones in the footwalls of the orebodies. The orebodies are zoned both vertically and laterally, having chalcocite cores surrounded by bornite-rich zones, passing out into narrow fringes of chalcopyrite and then into wide pyritic zones containing very minor sparsely disseminated pyrite (Fig. 22). Sulphur isotope values in the sulphides have a range in $\delta^{34}\text{S}$ of -2.3 to -16.0 permil CDT, and are interpreted to have resulted from thermochemical abiogenic reduction of sulphates at high temperatures (Master, 1991).

Copper mineralization occurs in several forms: (a) as even, banded or cloudy disseminations in arkose and schist; (b) as a replacement of detrital iron-titanium oxides on crossbed foreset laminae; (c) as syntectonic quartz-microcline-sulphide (-haematite-carbonate) veins occupying brittle fractures in competent lithologies; (d) as cleavage-parallel syntectonic quartz-microcline-sulphide veins in semi-pelitic schists. The ore textures are interpreted as the result of partial remobilization of pre-tectonic disseminated mineralization during polyphase deformation and metamorphism.

The stratabound mineralization at Mangula Mine, and the accompanying alteration, was produced by saline, slightly alkaline oxidising basin brines, which evolved through reaction with evaporites in the sequence, and which leached metals out of the redbeds, especially from detrital components like titanomagnetite, chromite, zircon, apatite and labile ferromagnesian minerals. The high copper and silver contents of the ores, the relatively low gold and platinoid contents, and the absence of lead and zinc are explained by the respective solubilities of these metals in the postulated ore fluids (Master, 1991). Sulphide precipitation occurred where mineralizing fluids encountered reduced beds and/or reduced fluids, and through replacement of pre-existing pyrite and magnetite.

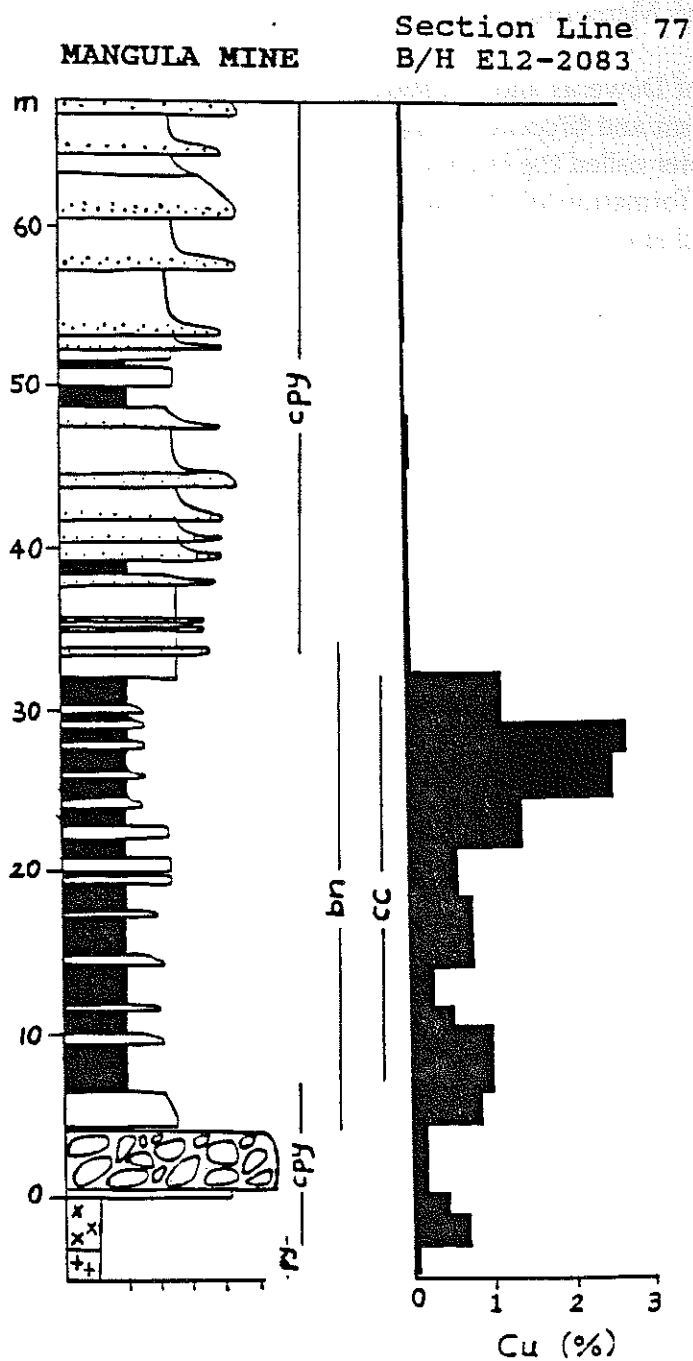


Figure 22: Mid Plate Orebody in borehole E12/2083 at Mangula Mine (after Master, 1991)

7.2: Highbury Meteorite Impact Structure

Exposures of Deweras and Lomagundi Group rocks which have undergone intense shock metamorphism and brecciation by a large meteorite impact, which produced a crater 20 km in diameter called the Highbury Impact Structure (Fig. 23). Shock metamorphic effects include the formation of Planar Deformation Features (PDFs) in quartz, which have an orientation characteristic of shock deformation at pressures exceeding 150 kbars (Fig. 25), and silica-rich impact glass (which has been partly devitrified). A granophyre exposed in the Ridziwi stream intrudes meta-arkoses and tremolitic marbles of the Deweras Group. This granophyre, which is interpreted to be an impact melt, has been dated at 1034 ± 13 Ma (Fig. 24, after Master et al., 1995).

Day 4

Stop 8 (Fig. 8): Shackleton-Avondale Cu-Ag Mine

Underground visit to Shackleton Mine (Fig. 26), which is hosted by metasedimentary rocks of the Deweras Group. In the Avondale section, will examine stratabound copper-silver orebodies hosted in conglomerates, arkoses and argillites. The orebodies at Shackleton and Avondale are in the form of elongate ore-shoots formed under impermeable and reducing argillite caps in doubly-plunging en-echelon anticlinal trap structures associated with a major sinistral wrench fault which was the feeder for the mineralizing brines (Fig. 27).

The Avondale sequence is separated from the overlying Shackleton sequence by the Dolomitic Argillites. Fresh exposures of these will be studied on 10 Level. The dolomitic argillites consist of thinly bedded dolomite horizons alternating with clastic ripple-marked dolomite and upward-fining marly arenite units. Thin pink anhydrite layers may overlie persistent chemically precipitated dolomite beds. The anhydrites are also reworked clastically into ripples. The ripple-marked dolomites exhibit the whole range of sedimentary structures indicative of tidal flat environments, including single, bifurcated and trifurcated flaser bedding, lenticular and wavy bedding, and starved ripples. Such structures are indicative of time-velocity asymmetry in the depositional environment, with alternating periods of ebb and flood flow (during which ripple marks form), separated by highstands and lowstands during which shale drapes form. Such processes are characteristic of a shoreline environment, which in this case was on the shores of a saline playa lake which deposited evaporites (carbonates and sulphates).

The Avondale orebody is associated with two or three argillite horizons (known as the Hangingwall, Middle and Footwall argillites), which occur with plane-bedded arenites interbedded with trough crossbedded arenites and conglomerates (Fig. 28). Mineralization is erratic, and may vary in its stratigraphic position with respect to the argillites- sometimes it is associated with one argillite, sometimes with another, and in other cases with

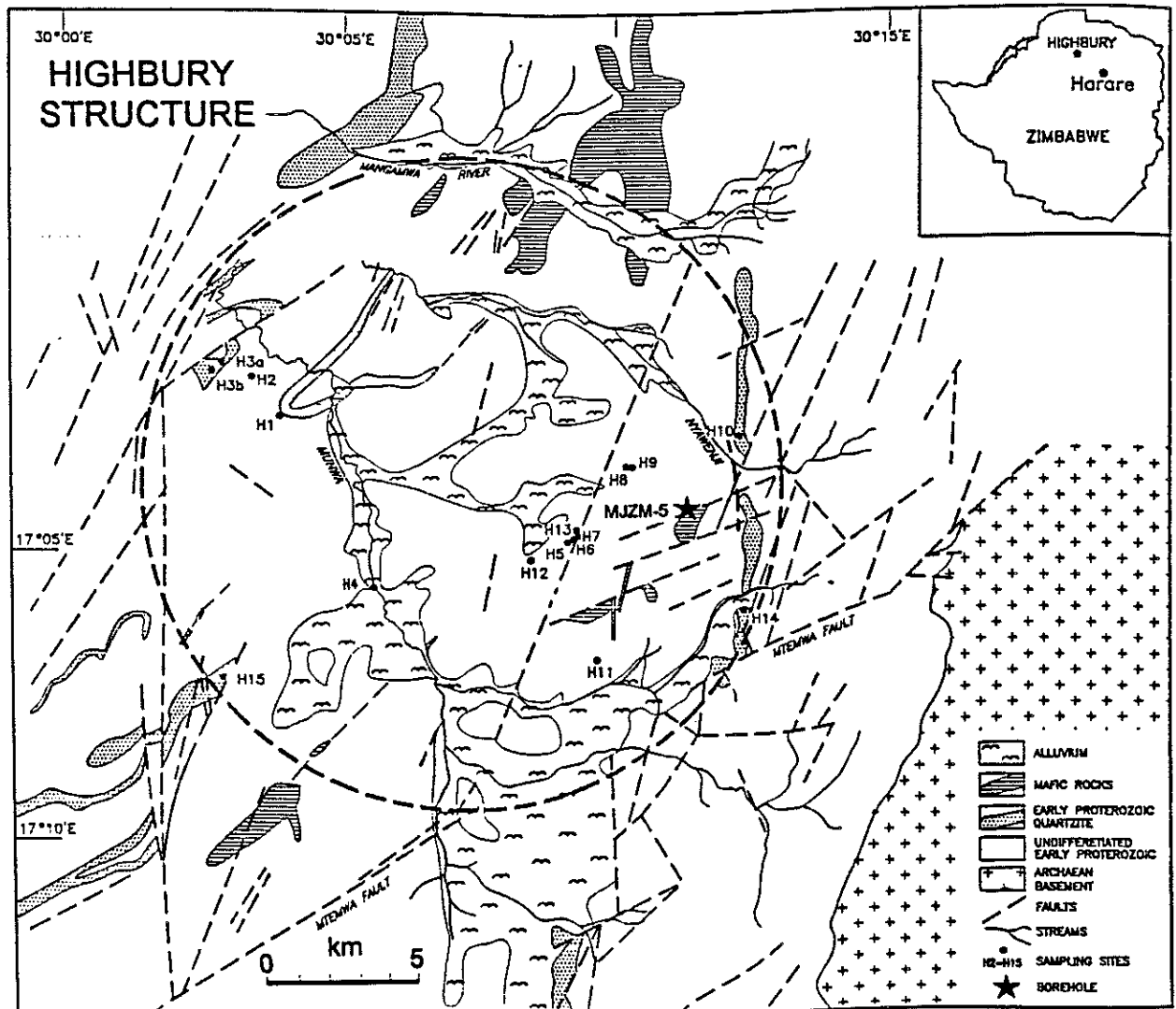


Figure 23: Simplified geological map of the Highbury Structure (dashed circle), after Stagman (1961) [6].

Figure 24: U-Pb plot of Munwa granophyre zircons. Euhedral (igneous) concordant zircons have an age of 1034 ± 13 Ma. Older xenocrystic detrital zircons (5.1, 5.2) show Pb-loss at the same time. Some younger zircons (eg. 12) show a Pb-loss (thermal) event at c. 216 Ma (Karoo?).

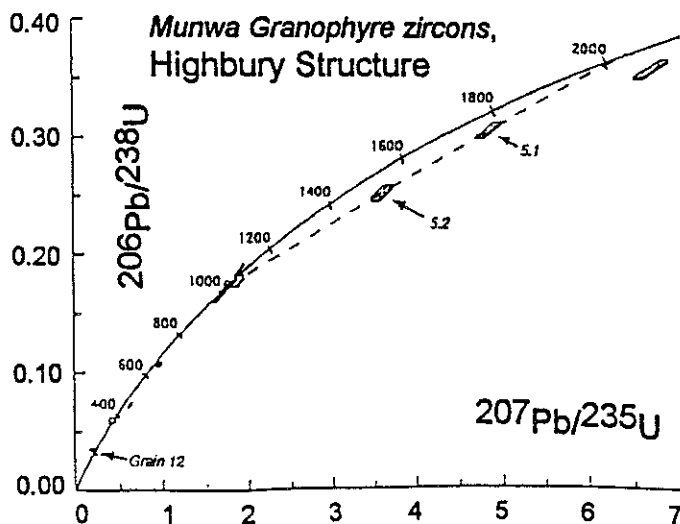
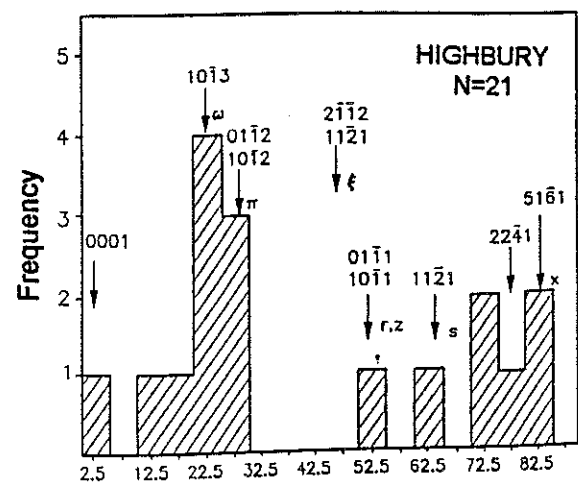


Figure 25: Histogram of orientations of PDFs in Highbury quartz (angle in degrees wrt 0001)



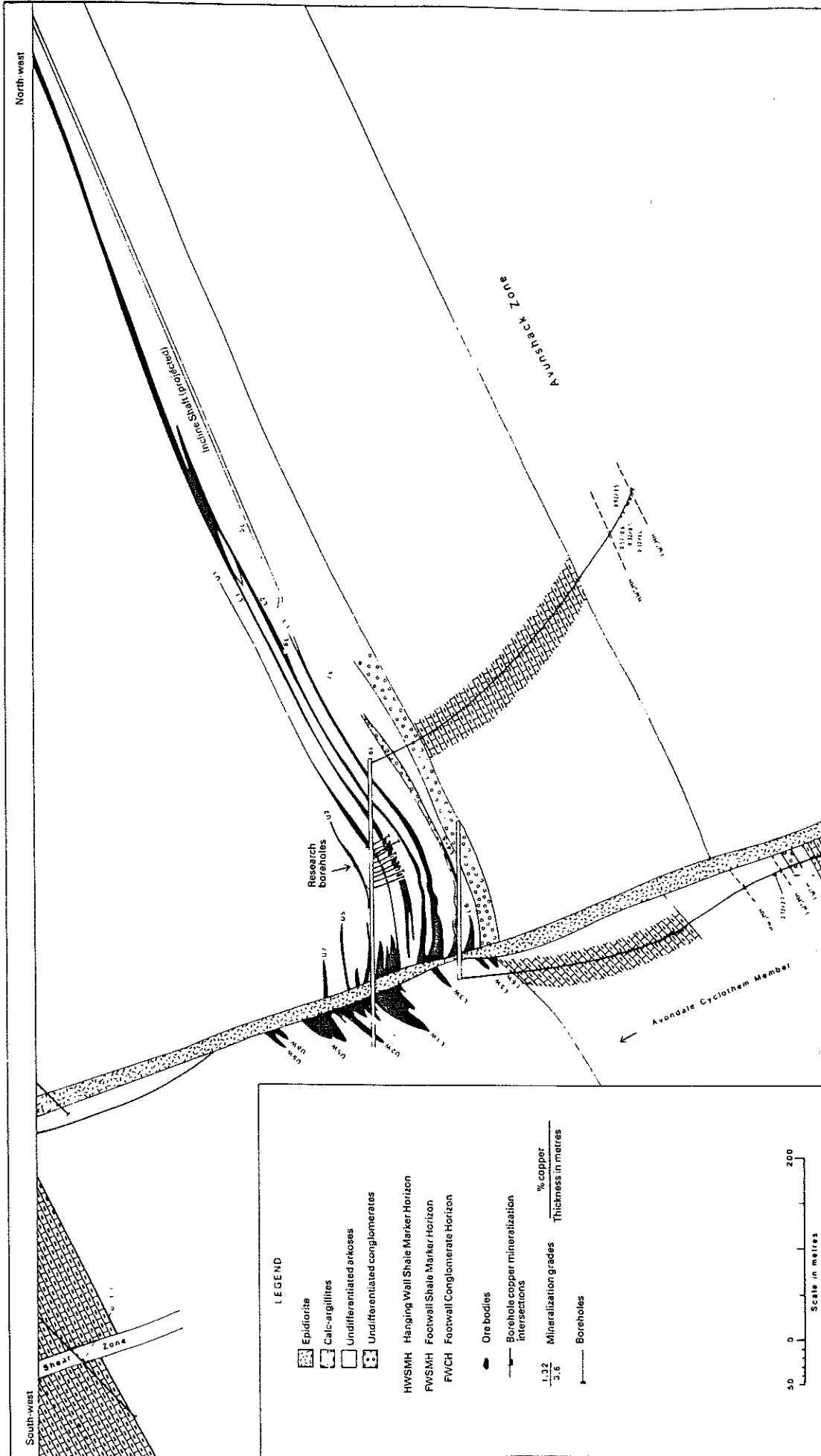


Figure 26: Longitudinal section of Shackleton Mine (after Newham, 1986).

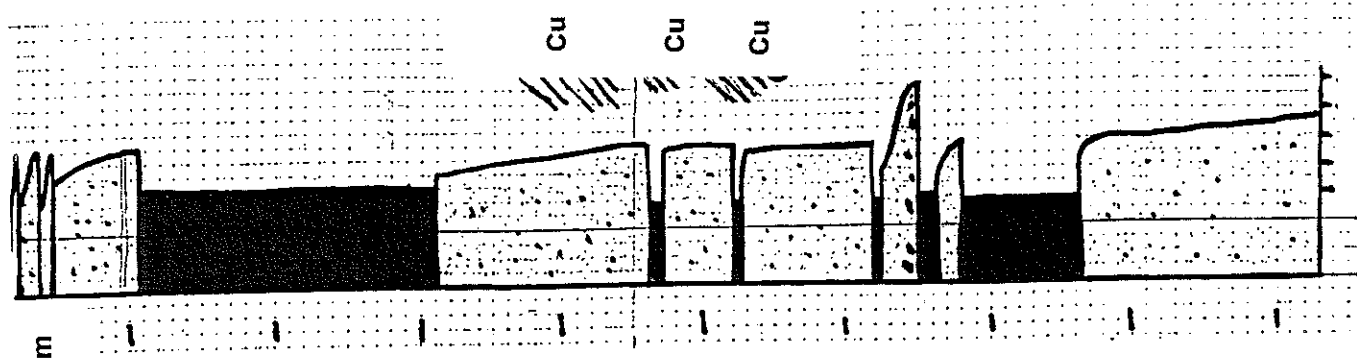


Fig. 28: Stratigraphic section through the Avonshack ore body on 10 Level, Shackleton Mine

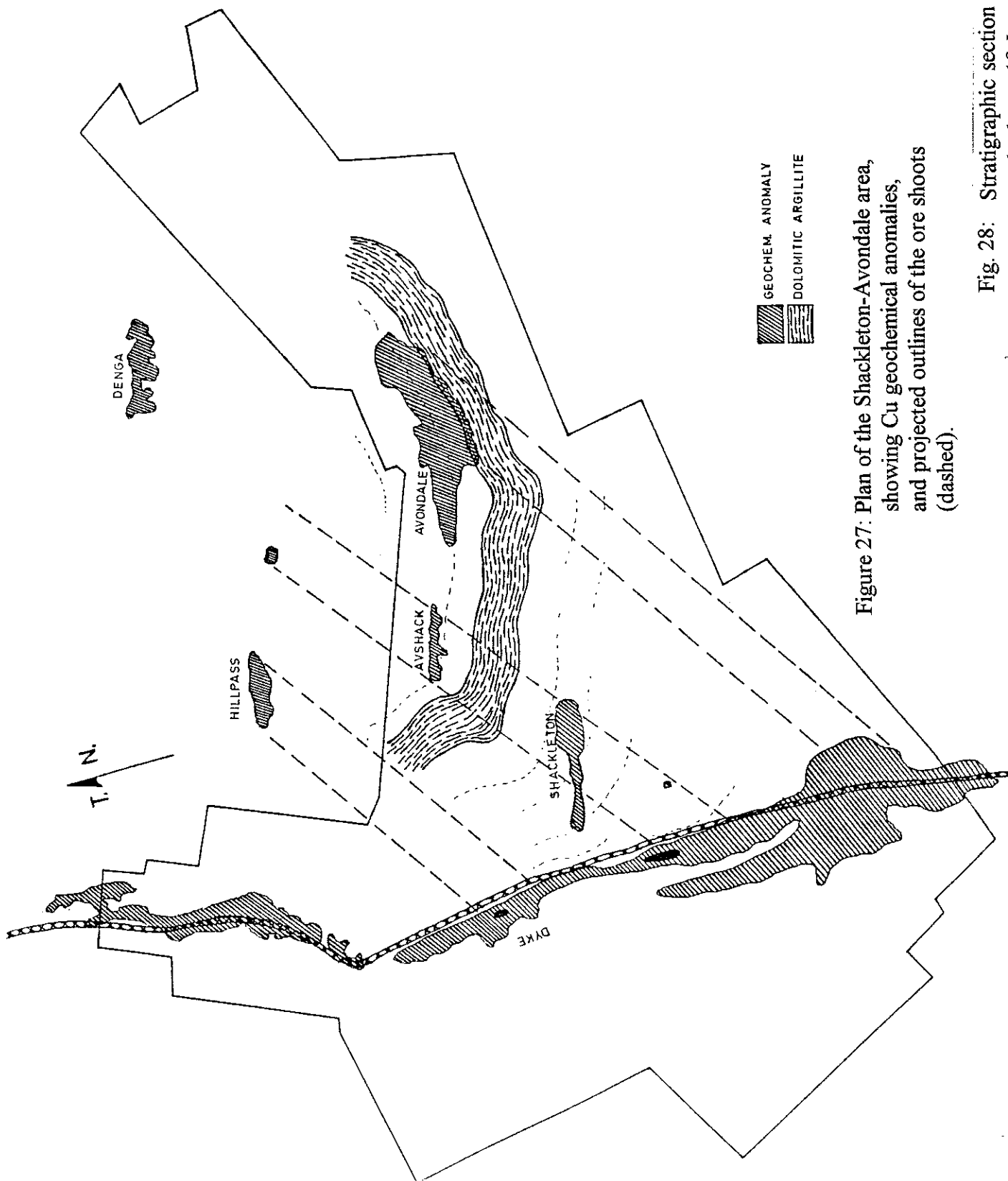


Figure 27: Plan of the Shackleton-Avondale area, showing Cu geochemical anomalies, and projected outlines of the ore shoots (dashed).

two or three argillites. The exact controls on the position of the mineralization are still unknown. The Avondale conglomerates are oligomictic, with mainly shale intraclasts and small granite clasts, which do not get beyond the pebble to cobble range in size. The argillite horizons are commonly mudcracked, and provide abundant intraformational clasts for the overlying conglomerates. Some of these clasts are imbricated, and show palaeocurrents trending towards the east. In the immediate footwall, stratigraphically below the Avondale ore horizons, there occur large-scale crossbedded arkosic arenites, which have been proven to be aeolianites. These have interbedded interdunal fan sediments consisting of mud-cracked argillites.

Stop 9 (Fig. 8): Muchi River thrust front

The thrust front of the Magondi Belt is exposed along the Muchi River (Fig. 29). Here Lomagundi group quartzites are thrust over the Archaean basement.

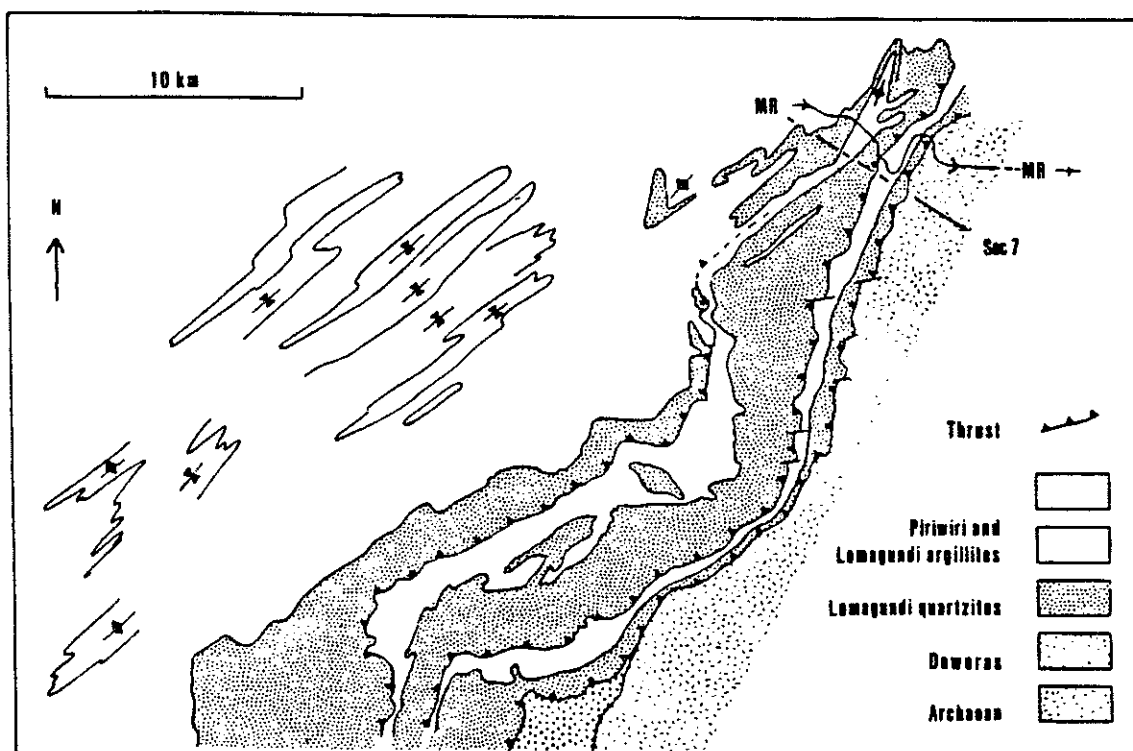


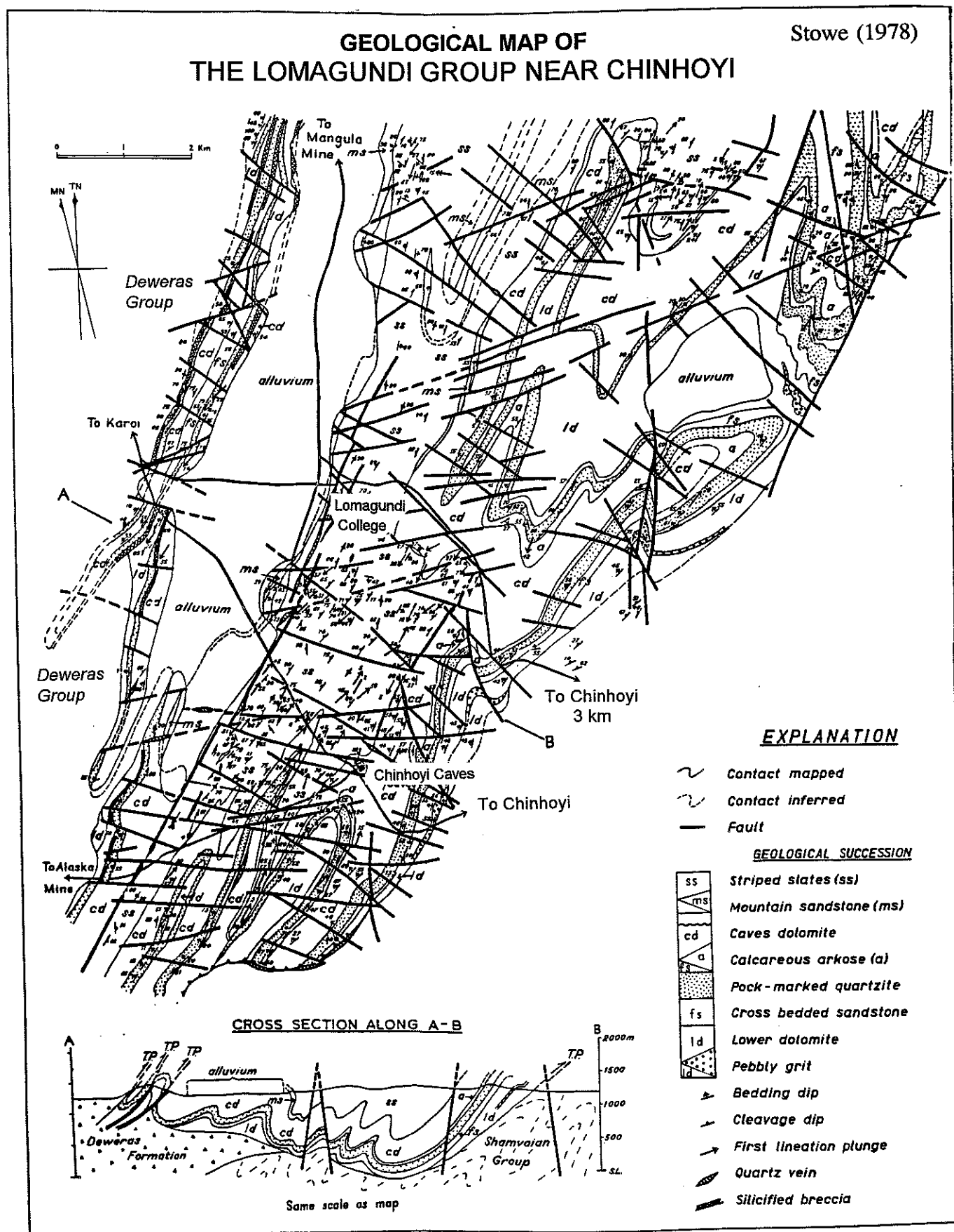
Figure 29: Map of the basal thrusts and overlying fold belt in the southern part of the Magondi Belt (after Tennick & Phaup, 1976; Treloar, 1988). MR = Muchi River

Day 5

Stop 10: Chinhoyi Caves (Fig. 30)

The spectacular Chinhoyi Caves, one of the biggest tourist attractions in Zimbabwe, are karstic features developed in the Lomagundi dolomites. The caves are situated along a

Figure 30: Geological map of the Lomagundi Group near Chinhoyi (after Stowe, 1978).



large fault zone in the dolomites. The Wonder Hole is a large karst sinkhole with circular outline, in the bottom of which is a 90 m-deep lake filled with clear, blue water.

10.1: Road Traverse, Lomagundi Group

Road traverse of lithologies of the early Proterozoic Lomagundi Group, along the Chinhoyi-Lomagundi College Road. This area was mapped by Stowe (1978) (Fig. 30). Along this traverse there are exposures of stromatolitic dolomites and Pockmarked Quartzite of the Mcheka Formation, and graphitic shales, Striped Slates and Mountain Sandstone of the Nyagari Formation.

Stop 11: Deweras Group aeolianites in Angwa River, on the road between Chinhoyi Caves and Alaska Mine. Large-scale planar crossbedded arkosic sandstones of the Deweras Group display small-scale features that are diagnostic of aeolianites, including cm-scale inversely-graded ripple-cross-laminated "subcritically-climbing translent strata" (Hunter, 1976), wedge-shaped massive grainflows (avalanche deposits), and pinstripe lamination. These are among the oldest authenticated aeolianites in the world (Master, 1995).

Stop 11.1: Visit to the Alaska Mine quarry, from which oxidised copper ore, mainly malachite, was mined for centuries by the indigenous population in the pre-colonial era.

The mineralization at Alaska Mine (Fig. 31) occurs in highly sheared dolomites and intercalated sandstones and siltstones of the Lomagundi Group, and consists mainly of oxidised malachite ore, with some hypogene chalcocite or djurleite which occurs as pseudomorphs after pyrite, and minor chalcopyrite (McCann, 1928; Stagman, 1961; Newham, 1986). Sulphur isotopes of the sulphides range in $\delta^{34}\text{S}$ from +8.1 to -2.0 permil CDT (von Rahden and de Wet, 1984). The malachite occurs as paint-like films along cleavage planes and fractures. Other oxide minerals recorded are chrysocolla, cornetite, plancheite, shattuckite diopside, cuprite and tenorite. Native copper occurs as dendritic crystals, and as sheets along fractures and faults. J.B.E. Jacobsen (1964) described the geology of the deposit, and interpreted the host rocks to be part of an allochthonous nappe that was bounded at the base by a major breccia zone. The nappe consisted of several imbricately stacked thrust sheets, in what would today be termed a duplex structure (Fig. 32). Newham (1986) reinterpreted the structure to be a simple syncline, as shown in his idealised cross-section of the deposit. This is at total variance with the detailed mapping of Jacobsen (1964) (Figs. 31 & 32), as well as with maps produced by the mine in 1970.

Examination of a sample from the sandstone orebody, which contains 'chalcocite' pseudomorphs after pyrite, revealed convincing evidence for the timing of the mineralization. The 'chalcocite' was shown by XRD to be the first occurrence in Zimbabwe of the closely related mineral djurleite ($\text{Cu}_{31}\text{S}_{16}$) (Master, 1991). The djurleites, pseudomorphous after cubic pyrite, are deformed into parallelepipeds, and appear diamond-shaped in cross section. The host rock is a highly sheared metasiltstone,

GEOLOGICAL SECTIONS THROUGH ALASKA AREA

Mapped by J. B. E. Jacobsen 1960

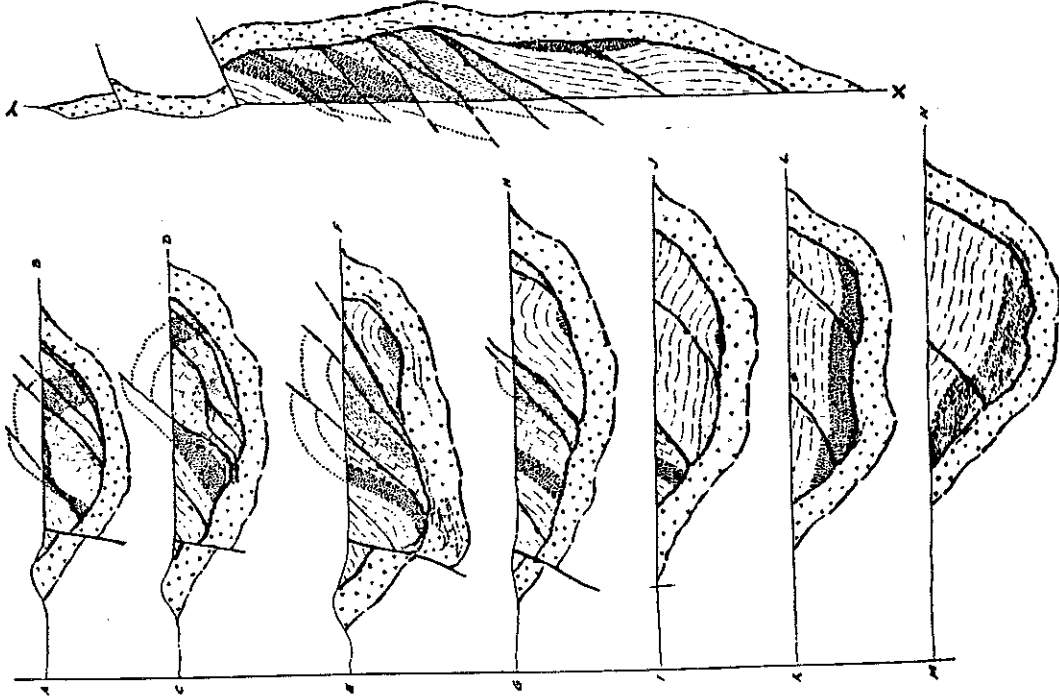


Fig. 32: Geological sections through Alaska Mine (after Jacobsen, 1964). The section lines are shown in Fig. 31.

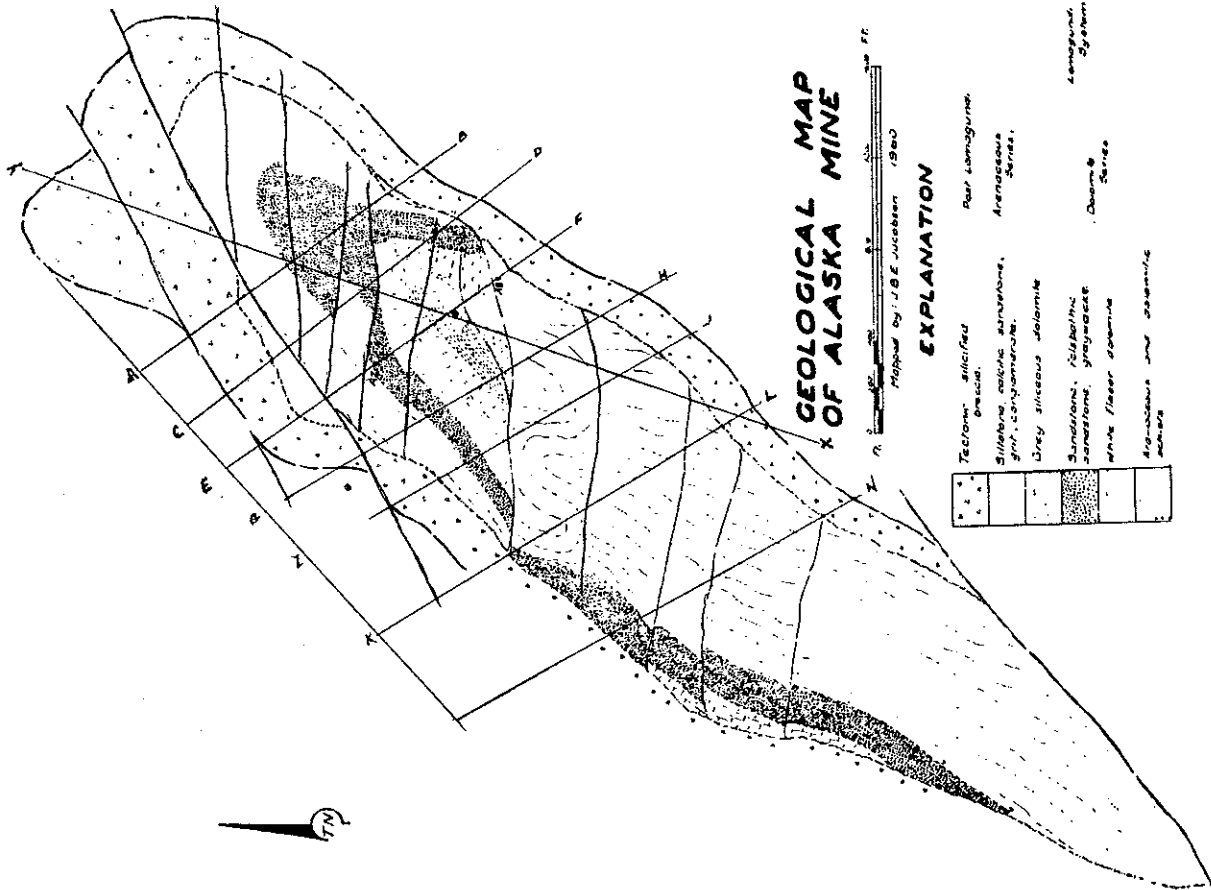


Figure 31: Geological map of Alaska Mine (after Jacobsen, 1964).

which has shear planes with talcose partings, and which have a strong slickensided striation lineation, with steps at right angles to this. Fibrous minerals growing in the lee of the slickenside steps are oriented parallel to the lineation. The long axes of the deformed djurleite pseudomorphs are also aligned parallel to the lineation, and they appear to have stretched during simple shear. The djurleite pseudomorphs have quartz-rich pressure shadow fringes, indicating that the replacement took place after these fringes had formed around the earlier euhedral pyrites. If the djurleite replacement had taken place before any deformation, there would be no pressure shadows around the djurleites, but instead, because of the low grain boundary energy and strength of chalcocites, they would have been totally flattened into parallelism with the cleavage. The deformed pseudomorphs with pressure shadows indicate that the replacement must have happened syntectonically. A first increment of deformation produced a schistosity in the rock, and formed quartz pressure shadows around rigid pre-existing pyrite crystals. The rock was then infiltrated syntectonically by copper-bearing solutions moving along permeable cleavage and fracture planes, which replaced the pyrite by djurleite. The djurleites, with their inherited quartz pressure shadow fringes, then underwent further deformation, in which they behaved plastically, and suffered rotation and flattening by simple shear. A similar example of chalcocite pseudomorphs after euhedral pyrite has been recorded from the Klein Aub Mine in Namibia (Borg, 1987), but in this case the replacement was post-tectonic, since the chalcocites, with their quartz pressure shadows, are undeformed.

Stop 11.2: Halite casts, Nyagari Formation

At 32 km along the road from Alaska to Sanyati, there is a roadcut with exposures of siltites of the Nyagari Formation, of the Lomagundi Group, which contain halite casts in the form of hopper crystals.

Day 6

Stop 12: Sanyati Mine (Cu-Zn-Pb-Ag Massive Sulphide deposits)

The Sanyati polymetallic Cu-Zn-Pb-Ag massive sulphide deposits are situated about 100 km SW of Chinhoyi. They are expressed on surface as a line of spectacular malachite-stained ferruginous gossans which extend from the Copper King Dome to the Copper Queen Dome, over a strike length of about 25 km (Fig. 33). The deposits, including the Copper Queen, Copper King, Copper Joker and Copper Straight prospects, which are all developed along the same strike, were first pegged in 1910, and briefly worked for copper in 1918-1919. They subsequently went through a checkered history, including a major share fiasco in the 1920's, before being acquired by MTD in the 1950's. The deposits were taken over by ZMDC when MTD withdrew from Zimbabwe in 1985. In 1994 Reunion Mining (Zimbabwe) formed a joint venture with ZMDC to mine the oxidised part of the deposit. The only prospect that has been extensively drilled and developed underground is the Copper Queen prospect (J-Lines) (Fig. 34), where about 14.2 million tonnes of ore, grading at about 1.2% Cu, 3.2 % Zn and 0.9% Pb, was proven.

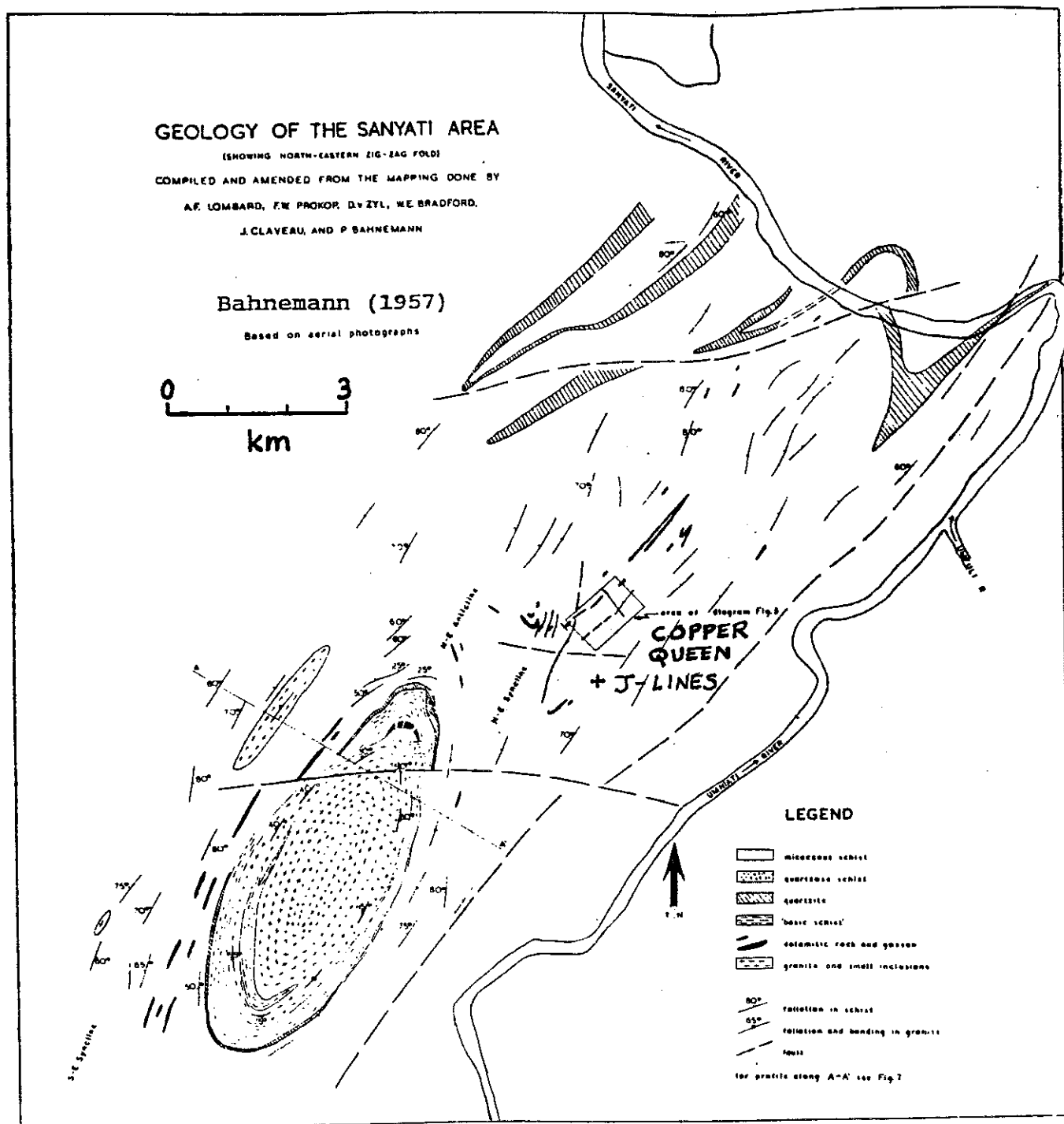


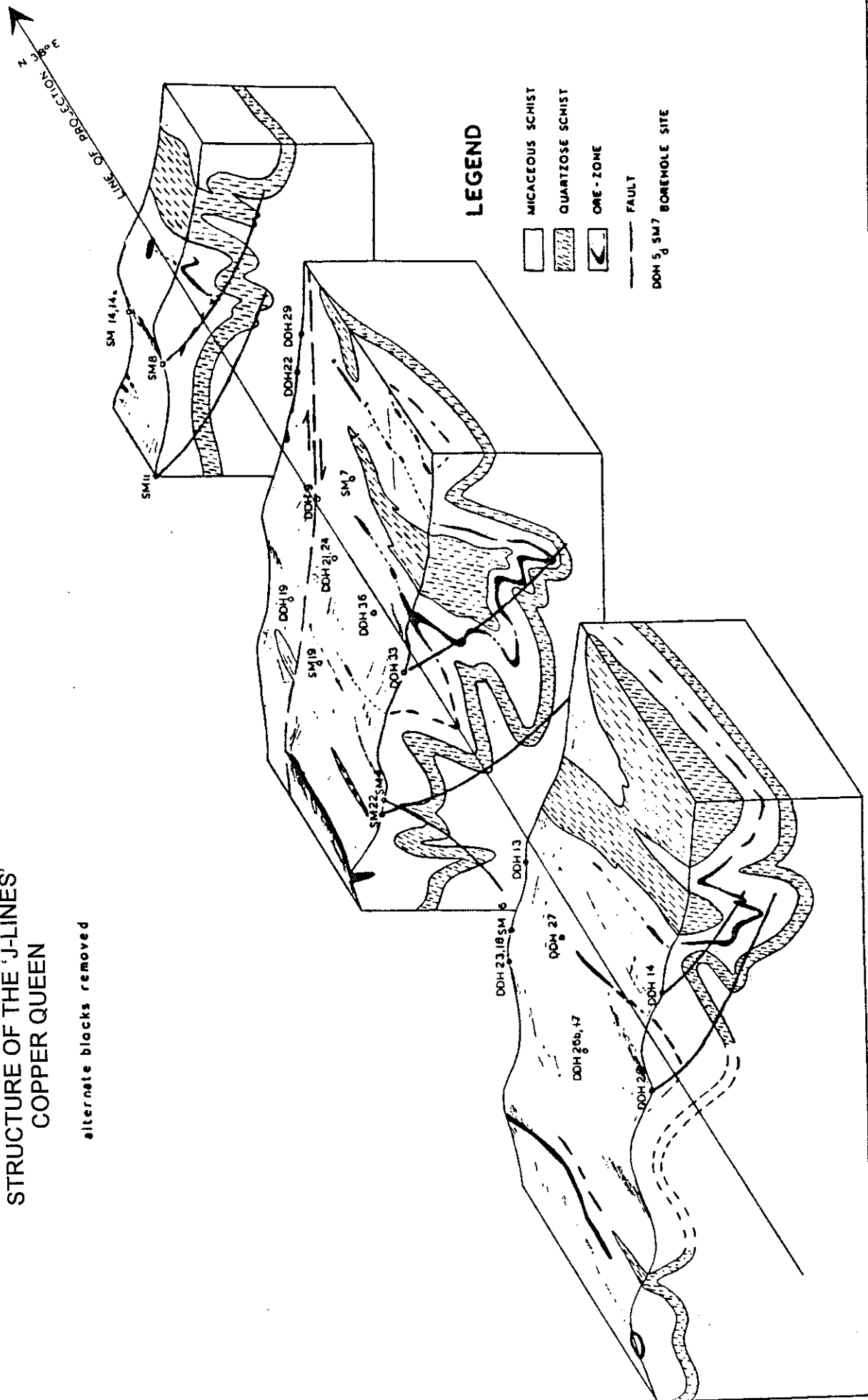
Fig 33: Geological sketch map of the Sanyati area (after Bahnemann, 1957).

Figure 34:

STRUCTURE OF THE 'J-LINES' COPPER QUEEN

alternate blocks removed

(Bahnmann, 1957)



The mineralization is closely associated with a band of tremolitic ferruginous dolomite marble which is surrounded by phyllites, schists and feldspathic quartzites. The hypogene ore minerals consist mainly of pyrrhotite, sphalerite, chalcopyrite, galena, arsenopyrite and pyrite, with minor magnetite, cubanite, valeriite and marcasite. Bahnemann (1957, 1961) suggested that the Sanyati deposits were skarn deposits related to emplacement of the Copper Queen and Copper King domes, but the style of mineralization shows great similarities with the class of sediment-hosted volcanogenic massive sulphide deposits referred to as "Besshi-type VMS" deposits. The continuity of the gossans over 25 km indicates that the Sanyati deposits have the potential to be a major ore district.

References

- Armstrong, I.H. (1975). Geology of the Lynx Graphite Mine. B.Sc. Spec. Hons. thesis (unpubl.), Univ. Rhodesia.
- Bahnemann, K.P. (1957). The ores of the "J-Lines", Sanyati Copper Mine, Southern Rhodesia. M.Sc. thesis (unpubl.), Univ. Pretoria.
- Bahnemann, K.P. (1961). The ores of the "J-Lines", Sanyati Copper Mine, Southern Rhodesia. Trans. geol. Soc. S. Afr., 44, 193-220.
- Bartholomew, D.S. (1990). Gold deposits of Zimbabwe. Geol. Surv. Zimbabwe, Mineral Resources Series No. 23, 75 pp.
- Bartholomew, D.S. (in prep.). The geology of the Doma North area. Bull. Geol. Surv. Zimbabwe.
- Borg, G. (1987). Controls on stratabound copper mineralization at Klein Aub Mine and similar deposits within the Kalahari Copperbelt of South West Africa/Namibia and Botswana. Ph.D. thesis (unpubl.), Univ. Witwatersrand, Johannesburg, 107 pp.
- Broderick, T.J. (1976). Explanation to the geological map of the country east of Kariba. Geol. Surv. Rhod. Short Rept. No. 43, 98 pp.
- Broderick, T.J. (1981). The Zambezi Metamorphic Belt in Zimbabwe, 739-743. In: Hunter, D.R. (Ed.), Precambrian of the Southern Hemisphere. Elsevier, Amsterdam, 822 pp.
- Chenjerai, K.G. (1988). A preliminary report on the geology north of Chenanga. Annals Geol. Surv. Zimbabwe, Vol. XIII 1987, 1-7.
- Condie, K.C. and Harrison, N.M. (1976). Geochemistry of the Archean Bulawayan Group, Midlands greenstone belt, Rhodesia. Precambrian Res., 3, 252-271.

- Davies, B.J. (1982). Geophysical prospecting methods for graphite at the Lynx Mine area. M.Sc (Expl. Geophys.) thesis (unpubl.), Univ. Zimbabwe.
- Hahn, L., Steiner, L., Bosum, W., Damaske, D., Höhndorf, A., Kreuzer, H., Ott, G., and Resch, M. (1990). Geology and mineral prospecting in the Makonde and Guruve Districts, Zimbabwe. Bundesanstalt für Geowissenschaften und Rohstoffe, Hannover, Technical Cooperation Project No. 8421703, File No. 106842, 295 pp.
- Harper, G. (1973). Metamorphism in the southern Urungwe district, norththwestern Rhodesia. Spec. Publ. geol. Soc. S. Afr., 3, 127-130.
- Hitchon, B. (1958). The geology of the Kariba area. Geol. Surv. N. Rhod., Report no.3.
- Jacobsen, J.B.E. (1964). The geology of the Alaska Mine, Southern Rhodesia, 353-366. In: Haughton, S.H.(Ed.), The Geology of Some Ore Deposits in Southern Africa, II, Geol. Soc. S. Afr., Johannesburg, 739 pp.
- Kirkpatrick, I.M. (1976). The geology of the country around Tengwe, Lomagundi District. Bull. Geol. Surv. Rhod., 75.
- Kirkpatrick, I.M and Robertson, I.D.M. (1987). A geological reconnaissance of the Makuti-Kariba road-1968. Ann. Geol. Surv. Zimbabwe, vol. XII 1986, 1-7
- Kukla, P.A. and Stanistreet, I.G. (1990). The Khomas Hochland accretionary prism of the Damara orogen, Central Namibia. Abstract, Geocongress '90, Geol. Soc. S. Afr., Cape Town, 309-312.
- Leyshon, P.R. (1973). Two granite-gneiss domes in the Copper Queen area, Rhodesia. Spec. Publ. geol. Soc. S. Afr., 3, 97-109.
- Loney P.E. (1969). The geology of the Kariba District, Rhodesia, with special reference to geochemistry and amphibolite petrochemistry. Ph.D. thesis (unpubl.), Leeds Univ. Abstract in 14th ann. Rep. res. Inst. Afr. geol., Univ. Leeds (1970), p.19.
- Master, S. (1991). The origin and controls on the distribution of copper and precious-metal mineralization at the Mangula and Norah mines, Mhangura, Zimbabwe. Ph.D. thesis, Univ. Witwatersrand, Johannesburg, 385 pp.
- Master, S. (1995). Alluvial fan, aeolian dune and evaporitic playa lake sedimentation, and syn-sedimentary tectonics in the Deweras Group (Zimbabwe): a 2 Ga-old analogue of the Dead Sea strike-slip basin. Centennial Geocongress Geol. Soc. S. Afr., 3-7 April 1995, Rand Afrikaans University, Johannesburg, South Africa, Extended Abstracts, II, 834-837.

- Master, S., Armstrong, R.A., Brandt, D., Ferraz, M.F.F., Gumede, T., Koeberl, C., Reimold, W.U., Robertson, D.J., Woldai, T. and Zeil, P. (1995). New geological, geophysical and remote sensing data from the Highbury impact structure, Zimbabwe. *Lunar and Planetary Science*, XXVI, 903-904.
- McCann, W.S. (1928). Unpubl. Rept. on Alaska Mine. Quoted in Tyndale-Biscoe and Stagman, 1958.
- Muchemwa, E. (1987). Graphite in Zimbabwe. *Geol. Surv. Zimbabwe Min. Res. Series* No. 20, 15 pp.
- Munyanyiwa, H. and Blenkinsop, T.G. (1992). The relationship between Magondi Mobile Belt (Ubendian) and the Zambezi Mobile Belt (Pan-African) in northern Zimbabwe. *Extended Abstracts, 16th Colloq. Afr. Geol., Mbabane, Swaziland*, 224-226.
- Munyanyiwa, H., Hanson, R.E., Blenkinsop, T.G. and Treloar, P.J. (1996, in press). Geochemistry of amphibolites and quartzofeldspathic gneisses in the Pan-African Zambezi belt, northwest Zimbabwe: evidence for bimodal magmatism in a continental rift setting. *Precambrian Res.*, 79.
- Newham, W.D.N. (1986). The Lomagundi and Sabi metallogenic provinces of Zimbabwe, 1351-1393. In: Anhaeusser, C.R. and Maske, S. (Eds.), *Mineral Deposits of Southern Africa, II*, *Geol. Soc. S. Afr.*, 2335 pp.
- Prost, A.E. (1982). A preliminary report on the geology of the country north of Centenary. *Ann. Zim. Geol. Surv.*, VII 1981, 20-27.
- Stagman, J.G. (1961a). The geology of the country around Sinoia and Banket, Lomagundi District. *Bull. Geol. Surv. S. Rhod.*, 49, 107 pp.
- Stowe, C.W., Hartnady, C.J.H. and Joubert, P. (1984). Proterozoic tectonic provinces of Southern Africa. *Precambrian Res.*, 25, 229-231.
- Treloar, P.J. (1988). Geological evolution of the Magondi Mobile Belt, Zimbabwe. *Precambrian Res.*, 68, 55-73.
- Treloar, P.J. and Kramers, J.D. (1989). Metamorphism and geochronology of granulites and migmatitic granulites from the Magondi Mobile Belt, Zimbabwe. *Precambrian Res.*, 45, 277-289.
- Tyndale-Biscoe, R. and Stagman, J.G. (1958). Copper deposits in Southern Rhodesia. *Joint Meeting, East-Central, West-Central and Southern Reg. Comm. Geol., C.C.T.A., Leopoldville*, 181-195.

- von Rahden, H.V.R. and de Wet, J.J. (1984). Copper mineralization at the Shackleton Mine, Zimbabwe: syngenetic or epigenetic? In: Wauschkuhn, A. et al. (Eds.), *Syngeneses and Epigenesis in the Formation of Mineral Deposits*, 192-211. Springer-Verlag, Berlin Heidelberg.
- Watkeys, M.K. (1984). The Precambrian geology of the Limpopo Belt north and west of Messina. Ph.D. thesis (unpubl.), Univ. Witwatersrand, Johannesburg, 349 pp.
- Wiles, J.W. (1961a). The geology of the Miami Mica Field. *Bull. Geol. Surv. S. Rhod.*, 51, 235 pp.
- Wiles, J.W. (1968). Some aspects of the metamorphism of the Basement Complex in the Sipolilo District. *Trans. geol. Soc. S. Afr.*, Annex., 71, 79-88.
- Wilson, J.F., Bickle, M.J., Hawkesworth, R.J., Martin, A., Nisbet, E.G. and Orpen, J.L. (1978). The granite-greenstone terrains of the Rhodesian Archaean craton. *Nature*, 271, 23-27.
- Workman, D.R. and Cowperthwaite, I.A. (1963). An occurrence of kyanite pseudomorphing andalusite, from Southern Rhodesia. *Geol. Mag.*, 100, 456-466.
- Worst, B.G. (1960). The Great Dyke of Southern Rhodesia. *Bull. Geol. Surv. S. Rhod.*, 47.



**UNIVERSITY OF THE WITWATERSAND
JOHANNESBURG**

**UNESCO/IUGS
International Geological Correlation Programme**



**IGCP PROJECT 363:
LOWER PROTEROZOIC OF SUB-EQUATORIAL AFRICA**

**FIRST FIELD MEETING
(ZAMBIA/ZIMBABWE, 14-30 SEPTEMBER 1996)**

**EXCURSION GUIDEBOOK:
PALAEOPROTEROZOIC OF ZAMBIA AND ZIMBABWE**

Edited by

SHARAD MASTER

Leader: IGCP Project 363

*(Economic Geology Research Unit, Department of Geology,
University of the Witwatersrand, P/Bag 3, WITS 2050,
Johannesburg, South Africa)*

**ECONOMIC GEOLOGY RESEARCH UNIT
INFORMATION CIRCULAR No. 302**

September, 1996

**IGCP PROJECT 363:
LOWER PROTEROZOIC OF SUB-EQUATORIAL AFRICA**

**FIRST FIELD MEETING
(ZAMBIA/ZIMBABWE, 14-30 SEPTEMBER 1996)**

**EXCURSION GUIDEBOOK:
PALAEOPROTEROZOIC OF ZAMBIA AND ZIMBABWE**

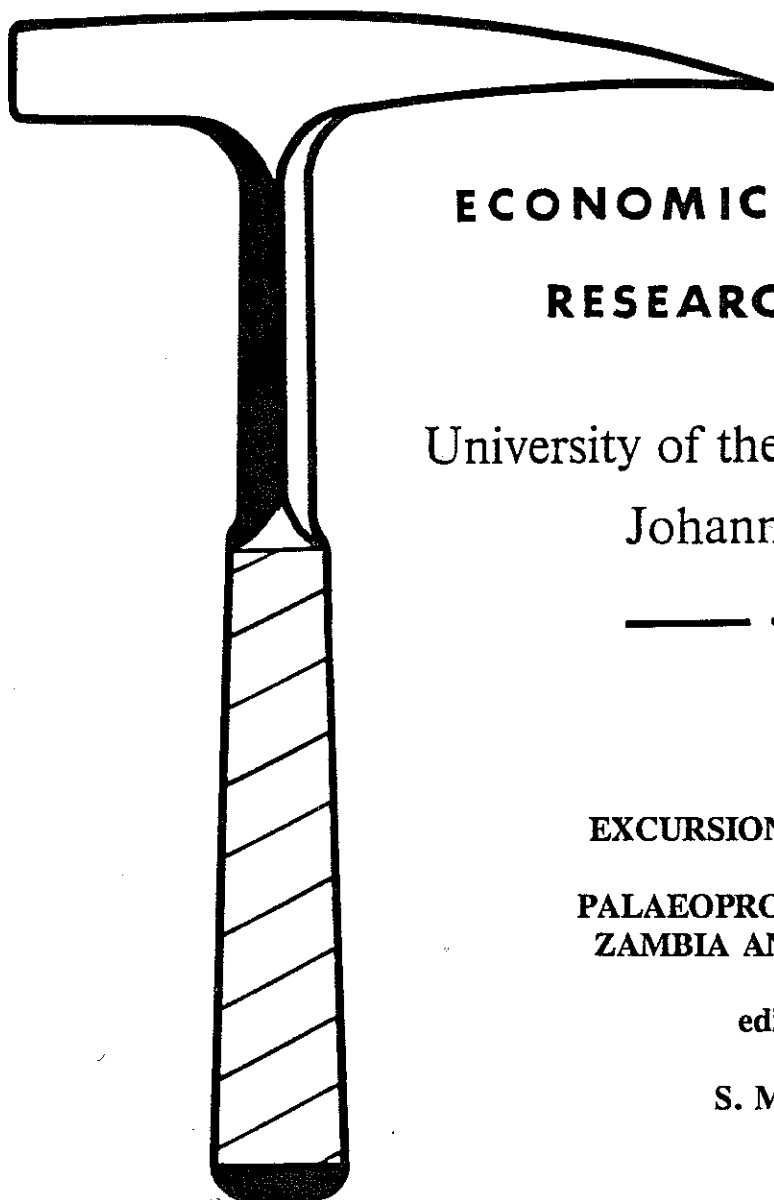
CONTENTS

	Page
<i>Pre-Conference Field Excursion:</i> Palaeoproterozoic of the Domes Area, Northwestern Zambia. F.Tembo, C.Namateba & S.Master	1
<i>Post-Conference Field Excursion No 1:</i> Palaeoproterozoic of Central and Eastern Zambia. F.Kamona, F.Tembo, O.Sikazwe, P.Siegfried & S.Master	12
<i>Post-Conference Field Excursion No 2:</i> The Palaeoproterozoic Magondi Mobile Belt, NW Zimbabwe S.Master	21

_____oOo_____

**Published by the Economic Geology Research Unit
Department of Geology
University of the Witwatersrand
1 Jan Smuts Avenue
Johannesburg 2001
South Africa**

ISBN 1 86838 232 X



**ECONOMIC GEOLOGY
RESEARCH UNIT**

University of the Witwatersrand
Johannesburg

EXCURSION GUIDEBOOK:

**PALAEOPROTEROZOIC OF
ZAMBIA AND ZIMBABWE**

edited by

S. MASTER

INFORMATION CIRCULAR No. 302